Omega xxx (xxxx) xxx

Contents lists available at ScienceDirect

Omega

journal homepage: www.elsevier.com/locate/omega

Optimal planning of the joint placement of photovoltaic panels and green roofs under climate change uncertainty

Mohammad Ramshani[a], Anahita Khojandi[a,*], Xueping Li[a], Olufemi Omitaomu[a,b]

[a] Department of Industrial and Systems Engineering, The University of Tennessee at Knoxville, Knoxville, TN 37996, US
[b] Urban Dynamics Institute, Oak Ridge National Laboratory, Oak Ridge, TN 37831, US

ARTICLE INFO

Article history:
Received 22 November 2017
Accepted 23 October 2018
Available online xxx

Keywords:
Stochastic optimization
Renewable energy generation
Energy savings
Climate change

ABSTRACT

Photovoltaic (PV) panels directly convert sunlight into electricity; but, sunlight also heats the panels, negatively impacting their efficiency. Green roofs are vegetative layers grown on rooftops, mainly to provide added insulation on the roof to save energy. Green roofs also cool near-surface air temperature. Hence, the joint installation of PV panels and green roofs may potentially lead to higher efficiency of PV panels in certain climates. We develop a two-stage stochastic programming model to optimally place PV panels and green roofs under climate change uncertainty to maximize the overall profit from energy generated and saved. We calibrate the model using the literature, industry reports, and the data from different, at times conflicting, climate projections. We then conduct a case study for a mid-size city in the U.S., perform extensive sensitivity and robustness analyses and provide insights.

© 2018 Elsevier Ltd. All rights reserved.

1. Introduction

Greenhouse gases are the most important contributing factor to the increase of average global temperatures over time [17]; at the current pace, it is estimated that the global temperature will rise by up to 5.8 °C over the next century [103]. Greenhouse gas emissions are primarily caused by burning fossil fuels [110] and without a significant change in energy production policies, specifically to reduce the reliance on fossil fuels, the current concentrations of greenhouse gases in the atmosphere is only expected to grow [67].

Solar power is a clean, free, and promising renewable energy source that helps reduce greenhouse gas emissions and hence, mitigate global warming and climate change. Photovoltaic (PV) panels, which can directly convert sunlight into electricity, are one of the most efficient methods of harnessing solar power. PV panels are the fastest growing renewable technology in the recent years at an annual average rate of 6.8% [45]. The number of panels installed within the U.S. increased by 63% between 2007 and 2008 [109], with an estimated increase of approximately 30% per year from 2013 through 2016 in the residential sector [45]. This rate of growth can be attributed to the decreasing costs of PV panels [52] as well as the incentives provided by state and federal governments. The falling prices of PV panels, coupled with the overall increases in power costs from conventional sources, suggest that PV panels are on track to become a strategically advantageous solution to sustainable energy production [132]. It is, however, important to note that despite the increase in demand and the popularity of PV panels, efficiency of PV panels is still limited and depend mainly on the panels' cell material and their operating temperature. The open circuit voltage shows a drop of 2.3 mV per 1 °C rise in temperature, which translates to a 0.5% drop in efficiency per degree Celsius rise in temperature [129]. While there is ongoing research into engineering solutions to increase the efficiency of PV panels, this paper explores an immediate operational solution through improved, systemic placement decisions.

According to the U.S. Energy Information Administration (EIA), 47.7% of the energy consumed by residential households and 34% of the energy used by the commercial sector is due to space conditioning (i.e., heating and cooling) [45]. Given an expected average growth rate of 0.4%–1.2% and 0.9%–1.1% in the residential and commercial sectors, respectively, it is estimated that by 2040 the number of residential households grows to 150 million and the commercial space increases to 110 billion square feet [45]. Hence, any reduction in the energy required for space conditioning can result in substantial cost/energy savings. Green roofs (GRs), which are vegetative layers grown on rooftops, can provide added insulation on the roof and cool near-surface air temperature through decreasing the absorption rate of solar radiation by the building structure [36]. This cooling effect can contribute to an approximately 30% drop in the surface temperature [36]. Several long-term studies are currently underway to quantify the thermal performance of GRs [94,117] as well as the relationship between GRs and energy sav-

* Corresponding author.
E-mail address: khojandi@utk.edu (A. Khojandi).

https://doi.org/10.1016/j.omega.2018.10.016
0305-0483/© 2018 Elsevier Ltd. All rights reserved.

Please cite this article as: M. Ramshani, A. Khojandi and X. Li et al., Optimal planning of the joint placement of Photovoltaic panels and green roofs under climate change uncertainty, Omega, https://doi.org/10.1016/j.omega.2018.10.016

Fig. 1. GR integrated PV panel installed over a rooftop in Hailey, Idaho [119].

ings [29,102] under different climatic conditions. So far, it is estimated that widespread installation of GRs throughout the U.S. can result in $7 - $10 billion in savings [36].

In addition to direct savings in space conditioning costs, GRs can contribute to energy production of PV panels if they are jointly installed. Specifically, GRs create a cool micro-climate in hot weather and reduce the temperature of their surrounding area. Hence, their joint installation with PV panels (Fig. 1) can help cool down the panels, allowing them to function at a higher efficiency. The increase in panel efficiency is consistently reported in the literature; however, the degree of this increase varies from one study to another, ranging between 0.08% and 8.3% across studies of various lengths, conducted in different climates [24,71,80,130].

The degree of benefit from PV panels and GRs highly depends on the weather and climate conditions of the location in which they are installed [102,129]. However, the information on how the weather and/or climate conditions evolve over time in specific regions/locations are limited and often unreliable. Indeed, although the global trend of climate change is consistently reported, in general there is no consensus among current climate projections and their evolution over time in specific regions/locations [76]. For instance, Fig. 2 presents the daily maximum and minimum temperatures for the City of Knoxville, Tennessee from ten different climate projections for the year 2030, provided by Oak Ridge National Laboratory's Urban Dynamics Institute (UDI) [122] and Oak Ridge National Laboratory's Climate Change Science Institute (CCSI) [20]. As seen in the figure, the projections can differ by up to approximately 25.4 and 37.1 degrees Celsius for daily maximum and minimum temperatures, respectively, in a given day. Hence, using each of these forecasts to guide future benefits of installing PV panels and GRs, either separately or jointly, may result in a different set of recommendations.

PV panels and GRs are relatively expensive and have long lifespans, and hence, they are both considered long-term investments. PV panels can generally retain a high efficiency of 80%-85% up to 20 years after installment [46]. Similarly, GRs are reported to last on the order of 40 years [91,99], almost twice as long as traditional roofs. Therefore, it is important to carefully plan such investments to maximize their expected return.

In this paper, we present an approach to consolidate a set of future climate projections when making long-term investment decisions on the installation of PV panels and GRs, from the perspective of a regional governing body. Specifically, we develop a two-stage stochastic programming model to determine the optimal placement of PV panels and GRs, either separately or jointly, among a set of candidate rooftops. Our objective is to maximize the profit from the energy generated and saved using these practices, considering the uncertainties in the future evolution of the climate and the positive interaction of PV panels and GRs in increasing PV panels' efficiency. We develop a profit-maximizing model to allow governing bodies and policy makers to carefully evaluate their options before making an investment.

Optimal placement problems are studied in a wide array of domains and applications (e.g., for the placement of distributed generation source [125], phasor measurement units [58], multiple allocation hubs [31], and wind turbines [90], or in facility location problems [2]). In this paper, we formulate an optimal placement problem for joint installation of PV panels and GRs. In the literature, studies involving PV panels mostly focus on underlying PV material or cell technology [26,77,121]. Alternatively, there is a body of work that aims to determine the best placement option for individual PV panels. For instance, there are a number of studies that evaluate rooftop characteristics to calculate individual rooftop solar access using geographic information system (GIS) [84,96,123,128], or aim to develop GIS-based models to optimize electricity generation estimation of PV panels installed on rooftops [68].

Additionally, there exist studies whose objectives are to find the optimal installation criteria for PV panels, e.g., size, tilt angle, converter properties. An integrated multi-objective optimization model is developed in [81] to determine rooftop-specific installation criteria for PV panels to maximize their energy production effectiveness and efficiency. Similarly, a particle swarm optimization algorithm is developed in [82] to find the optimal installation details (i.e., number of PV modules, their optimal tilt angle and distribution among the DC-AC converters) for a grid-connected PV system to maximize the total net profit and environmental benefits of the system. In another study [86], a simulation model is developed to find the optimal size and slope of PV systems under certain climate conditions subject to equipment costs as well as electricity and sale-back tariffs. In a similar vein, in [25], a Bayesian approach is used to optimally size stand-alone PV systems under climate change uncertainty.

There exist only a few large scale studies that attempt to optimize the implementation of PV panels. In [6], the output of large scale renewable energy farms (both wind and solar) is evaluated and compared with that of rooftop PV panels, after minimizing energy generation costs and greenhouse gas emissions. In another study [98], the optimal strategy to implement PV systems to achieve national carbon emission reduction targets is proposed. None of these large scale studies, however, consider future climate scenarios to capture the uncertainty in output of PV panels, nor do they take into account GRs, their energy saving properties, or their interactions with PV panels.

The literature related to GRs mainly focuses on their many potential environmental benefits, e.g., management of runoff water quality and quantity [14], reduction of heat island and improvement of urban comfort [108], contribution to plant and ecological diversity [30], and reduction of urban air pollution [133], to name a few. Also, a major group of studies explore GRs' physical properties, e.g., types of substrate [5], hydrologic performance [85], thermal behavior [94], and vegetation types [113].

There exits a few studies in the literature that attempt to optimize energy savings/cost reductions achieved using GRs. For instance, Ramshani et al. [57] simulate the thermal behavior of a building covered with GRs in order to optimize the energy savings achieved by installing green media on the rooftop of a building. The results show that the installation of GRs for buildings that meet the most recent insulation regulations leads to moderate levels of energy savings. In another study, Kim et al. [78] investigate the economic and environmental benefits of GRs through an optimal-scenario selection model. The authors preform life-cycle cost analysis for fifteen different types of GRs and conclude that the cost reductions and environmental benefits achieved by GRs

Please cite this article as: M. Ramshani, A. Khojandi and X. Li et al., Optimal planning of the joint placement of Photovoltaic panels and green roofs under climate change uncertainty, Omega, https://doi.org/10.1016/j.omega.2018.10.016

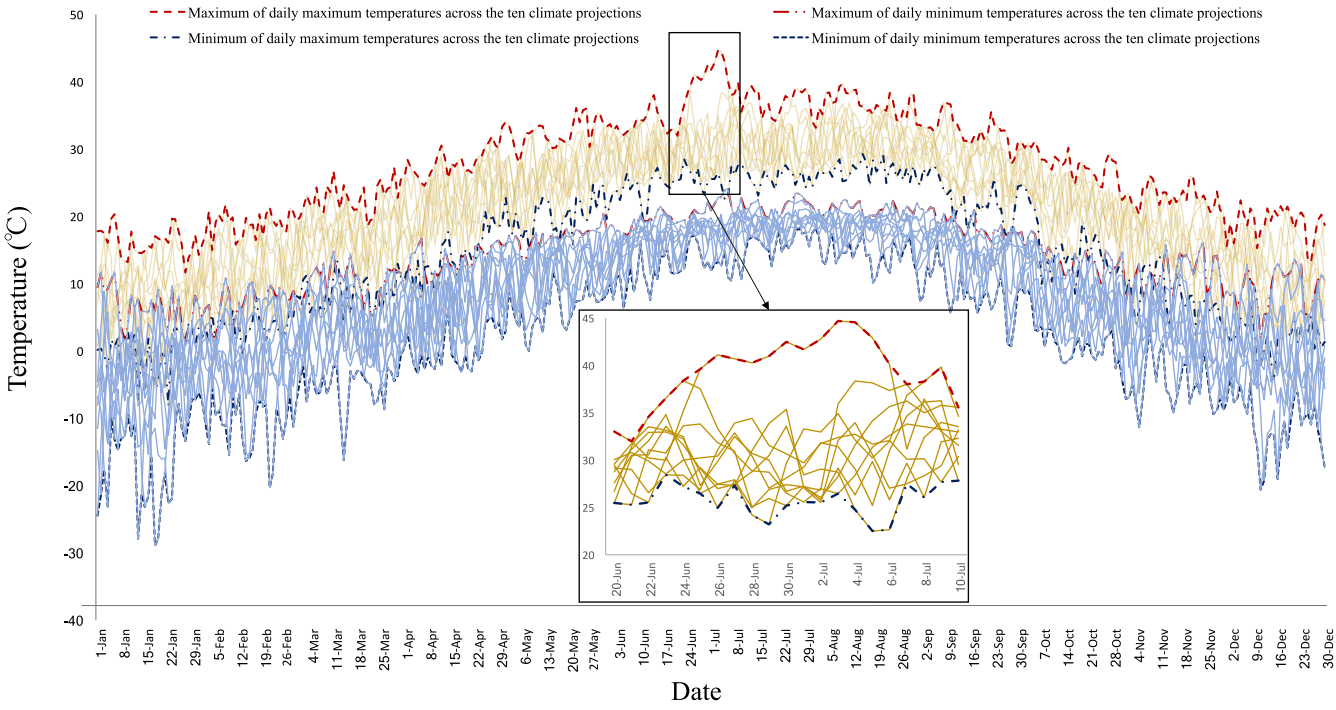
Maximum of daily maximum temperatures across the ten climate projections
Minimum of daily maximum temperatures across the ten climate projections
Maximum of daily minimum temperatures across the ten climate projections
Minimum of daily minimum temperatures across the ten climate projections
Temperature (°C)
Date

Fig. 2. The daily maximum and minimum temperatures for the City of Knoxville, Tennessee from ten different climate projections for the year 2030. The dashed lines present the maximum and minimum temperatures across the ten projections over the year. (For details on the climate projections refer to Table 3.).

are noteworthy. Chang et al. [23] conduct a cost-benefit optimization on GR sizes. Their results show that the amount of energy savings increases in the size of GR. Despite their contributions, none of these studies, however, examine the optimal placement of GRs in a large scale study.

Stochastic programming has been extensively used in the literature for modeling long-term planning problems under uncertainty [16]. Specifically, two-stage stochastic programming has been widely applied in a variety of studies including but not limited to portfolio selection [1], transportation planning [11], disaster management [95], waste management [89], scheduling [97], and distributed energy systems [136]. Similar to other works in the literature, here we aim to incorporate uncertainty about the future through a set of possible scenarios. However, to the best of our knowledge, this is the first study that uses such approach for incorporating climate change into urban planning over a long planning horizon.

Various cities or states in the U.S. have invested in, or are currently leading, projects to place green infrastructure and/or energy-efficient practices and technologies [49,50,120]. Most of these projects, however, are focused on investing in a single geographic region or a small community, and involve a single type of practice alone (e.g., solar panels, LED lights, green infrastructure). In this study, we take a forward-looking view and provide a general model that can account for joint placement of GRs and PV panels across various geographical regions simultaneously. To the best of our knowledge, this is the first model that accounts for multi-region, multi-practice placement, hence allowing policy makers to plan large-scale implementations, while accounting for the potential interactions between the practices.

The remainder of this paper is organized as follows. First we clearly define the scope of the problem and present the model formulation in Section 2. Next, in Section 3, we calibrate the model using the literature, industry reports and a few datasets. In Section 4, we first discuss the solution approach. Next we conduct a case study for a mid-sized city in the U.S., namely, Knoxville, Tennessee, perform sensitivity and robustness analyses, and provide environmental insights. Lastly, we conclude in Section 5.

2. Model formulation

In this section, we present a two-stage stochastic programming model with complete recourse to determine the placement of PV panels and GRs to maximize the overall profit. The first stage decisions are to choose a set of candidate sites to install PV panels and GRs, either separately or jointly. After all uncertainties are realized, second stage decisions, i.e., the amount of electricity sold to or purchased from the grid, are made. Note that consistent with the current practice, we assume that excess energy generated by PV panels can be sold to the grid [10]. In the remainder of the paper, the word*energy* refers to electrical energy unless otherwise stated.

Let T denote the planning horizon and K denote the set of regions, where I^κ denotes the set of candidate sites within region $\kappa \in K$. Let the discrete random variable W with probability mass function p_W denote the sample path of the future climate evolution for the regions of interest over the planning horizon. Let η_ω denote the realization probability of scenario $\omega \in \Omega$, where Ω is a finite discrete set of projected climate scenarios, i.e., $\eta_\omega = p_W(\omega)$.

Let the first stage binary variables x_i^κ and y_i^κ denote whether or not PV panels and GR are installed at candidate site $i \in I^\kappa$, respectively, where each assumes the value 1 if the corresponding practice is installed at site $i \in I^\kappa$ and equals to 0, otherwise. Let k_i^κ denote the total area of PV panel installed at site $i \in I^\kappa$. Let c_i^κ and g_i^κ denote the cost of installing PV system and GR at site $i \in I^\kappa$, respectively.

Let the second stage variables $e_{i\omega}^\kappa$ and $s_{i\omega}^\kappa$ denote the amount of energy generated and saved in kWh at candidate site $i \in I^\kappa$ under scenario $\omega \in \Omega$, respectively. Additionally, let H_i^κ denote the average hourly electricity consumption at each candidate site $i \in I^\kappa$ to maintain the building temperature via air conditioning, and R^κ denote the total required electricity for space conditioning in region $\kappa \in K$

Please cite this article as: M. Ramshani, A. Khojandi and X. Li et al., Optimal planning of the joint placement of Photovoltaic panels and green roofs under climate change uncertainty, Omega, https://doi.org/10.1016/j.omega.2018.10.016

over the planning horizon. Let δ denote the percentage change in energy consumed for space conditioning over the planning horizon, due to an array of technological, sociological, climatic, and economic factors. Lastly, let B denote the initial budget available for investment.

PV panels rely on solar irradiation to generate electricity and their outputs significantly differ depending on the number of hours they are exposed to sunlight. A 'peak sunlight hour' is typically used to describe the intensity of sunlight in a specific area , where 1 peak sunlight hour is equivalent to 1 kWh/m^2 [8,115]. Hence, the number of peak sunlight hours for a day represents the accumulative solar irradiation over the course of the day.

Additionally, the level of solar radiation received by any rooftop depends on a variety of factors, e.g., aspect of the building, rooftop slope, and the shadowing effect or solar access to buildings. Let ι_i^κ denote the rooftop solar radiation potential at site $i \in I^\kappa$, which quantifies the percentage of daily available sunlight that an average rooftop at site $i \in I^\kappa$ receives. Let the stochastic parameter L_ω^κ denote the total number of peak sunlight hours available over the planning horizon in region $\kappa \in K$ under scenario $\omega \in \Omega$.

Cooling and heating degree-hours are measures of how many degrees and for how long the outside temperature is above or below certain base temperatures, respectively [35]. These metrics are typically used to determine whether or not space heating and cooling are required for buildings. Let λ_ω^κ and τ_ω^κ denote the total number of cooling and heating degree-hours over the planning horizon, during which space cooling and heating are required, respectively, for buildings in region $\kappa \in K$ under scenario $\omega \in \Omega$. Additionally, let α and β denote the percentage of energy saving due to GR installation in cooling and heating degree-hours, respectively. Lastly, recall that the joint installation of PV panels and GRs positively affect the PV panels output. Let θ denote the percentage increase in the output of PV panels as a result of their integration with GRs. Table 1 summarizes all the notation used in model formulation.

Recall that our objective is to maximize the profit from energy generated and saved, i.e.,

$$Z = \max \sum_i \sum_\kappa -(Fx_i^\kappa + k_i^\kappa V^\kappa + A_i^\kappa P^\kappa y_i^\kappa) + \sum_\omega \sum_\kappa \eta_\omega (r_\omega^\kappa \mu - \phi_\omega^\kappa \gamma). \quad (1)$$

The first term inside the maximization corresponds to the installation cost of PV panels and GRs in a subset of candidate sites across all regions. The second term inside the maximization corresponds to energy generated and saved under all scenarios across all regions. The following equations, i.e., Eqs. (2)–(9), present the constraints of the model,

$$g_i^\kappa = A_i^\kappa P^\kappa y_i^\kappa \qquad \forall\, i, \kappa, \quad (2)$$

$$c_i^\kappa = Fx_i^\kappa + k_i^\kappa \left(V^\kappa + \mathbb{C}^\kappa\right) \qquad \forall\, i, \kappa, \quad (3)$$

$$\sum_i \sum_\kappa (c_i^\kappa + g_i^\kappa) \le B, \quad (4)$$

$$k_i^\kappa \le A_i^\kappa x_i^\kappa \qquad \forall\, i, \kappa, \quad (5)$$

$$e_{i\omega}^\kappa = QL_\omega^\kappa k_i^\kappa \iota_i^\kappa (1 + y_i^\kappa \theta) \qquad \forall\, i, \omega, \kappa, \quad (6)$$

$$s_{i\omega}^\kappa = H_i^\kappa y_i^\kappa (\alpha \lambda_\omega^\kappa + \beta \tau_\omega^\kappa) \qquad \forall\, i, \omega, \kappa, \quad (7)$$

$$\sum_i \left(e_{i\omega}^\kappa + s_{i\omega}^\kappa\right) + \phi_\omega^\kappa - r_\omega^\kappa \ge (1+\delta) R^\kappa \qquad \forall\, \omega, \kappa, \quad (8)$$

$$r_\omega^\kappa \le \sum_i e_{i\omega}^\kappa \qquad \forall\, \kappa, \omega. \quad (9)$$

Consistent with the literature [29,36,102], we assume that if the decision is to install GR at site $i \in I^\kappa$, it must be large enough to completely cover the rooftop; hence, Eq. (2) calculates the GR installation cost at site i in region κ. Eq. (3) links the PV system cost, c_i^κ, to its two different components, namely, PV system fixed cost, denoted by F, and PV system variable and maintenance costs in region κ, denoted by V^κ and $\mathbb{C}^\kappa$, respectively. Note that PV panels require very little maintenance [18,126], while extensive GRs are essentially cost-saving compared with conventional roofs when it comes to maintenance [60,63,131]. In this study, we assume the property owner is responsible for maintenance costs, whether or not their properties are selected by the model as candidates for placement of the green practices, i.e., $\mathbb{C}^\kappa = 0$. We revisit this assumption in our computational study in Section 4.3 to investigate the impact of incorporating maintenance costs directly into the model.

Eq. (4) limits the total cost of PV systems and GRs to a given budget B. Eq. (5) guarantees that the area covered with PV panels cannot exceed the available rooftop surface. Note that simultaneous installation of PV panels and GRs on a rooftop is possible as PV panels are generally installed slightly elevated above the roof surface.

Recall that the integration of PV panels and GRs can help cool down the panels, thereby resulting in a higher electricity output. Therefore, Eq. (6) calculates the energy generated by PV panels at site $i \in I^\kappa$ under scenario $\omega \in \Omega$.

The amount of energy savings from GR at each candidate site is given by Eq. (7). The amount of electricity sold to or purchased from the grid, r_ω^κ and ϕ_ω^κ, respectively, serve as second stage decisions in the model. We assume that each region has certain energy requirements for space conditioning over the planning horizon. Hence, Eq. (8) guarantees that for each region the total energy generated, $e_{i\omega}^\kappa$, and saved, $s_{i\omega}^\kappa$, and the total electricity sold to the grid, r_ω^κ, or purchased from the grid, ϕ_ω^κ, is at least equal to the energy requirement for space conditioning of the region. Lastly, Eq. (9) assures that the electricity sold to the grid cannot exceed the electricity generated by systems.

Note that the placement problem (1)–(9) has complete recourse. That is, for all the first-stage decisions, regardless of the uncertainties, there exists at least one feasible second-stage decision [16].

3. Model calibration

In this section, we use the literature and a series of datasets to calibrate the model formulated in Section 2 to further conduct a case study for the City of Knoxville, Tennessee.

3.1. Parameters estimated from the literature

In the following, we use the literature and industry reports to estimate model parameters.

Planning horizon, T. In this paper, we use two planning horizons of 10 years and 20 years. These two horizons are chosen based on the availability of future climate projections as well as the lifespan of current commercially available PV panels and GRs.

PV system fixed cost, F, and PV system variable cost in region κ, V^κ. The cost of installing PV system includes the workforce cost, plus the costs of the system components, i.e., solar modules (which is referred to the PV cell circuits sealed in an environmentally protective laminate [54]), mounting device, DC-AC power inverter, and wiring. Note that both workforce and component costs consist of fixed costs and variable costs, i.e., some of these costs are fixed for

Table 1
Notation used in the model.

Sets	
Ω	Set of climate scenarios, where $\omega \in \Omega$
K	Set of regions, where $\kappa \in K$
I^κ	Set of candidate sites in region $\kappa \in K$, where $i \in I^\kappa$
First stage variables	
x_i^κ	Equals 1 if PV panels are installed at site i in region κ and 0, otherwise
y_i^κ	Equals 1 if GR is installed at site i in region κ and 0, otherwise
c_i^κ	Installation cost of PV system at site i in region κ (USD)
g_i^κ	Installation cost of GR at site i in region κ (USD)
k_i^κ	Area of PV panel installed at site i in region κ (m^2)
Second stage variables	
$e_{i\omega}^\kappa$	Energy generated by PV panels at site i in region κ under scenario ω (kWh)
$s_{i\omega}^\kappa$	Energy saved by GR at site i in region κ under scenario ω (kWh)
r_ω^κ	Energy sold to the grid in region κ under scenario ω (kWh)
ϕ_ω^κ	Energy purchased from the grid in region κ under scenario ω (kWh)
Parameters	
F	PV system fixed cost (USD)
Q	PV panel output (W)
B	Initial budget available for investment (USD)
γ	Cost per kWh purchased from the grid (USD)
μ	Price per kWh sold to the grid (USD)
α	Percentage energy saving in cooling degree-hours due to GR installation
β	Percentage energy saving in heating degree-hours due to GR installation
θ	Percentage efficiency increase in the output of PV panels due to integration with GRs
δ	Percentage change in energy consumed for space conditioning over the planning horizon
V^κ	PV system variable cost in region κ (USD)
$\mathbb{C}^\kappa$	Total maintenance cost per m^2 PV panel installed in region κ (USD)
P^κ	Cost per m^2 for installing GR in region κ (USD)
R^κ	Total energy requirement for space conditioning in region κ over the planning horizon (kWh)
η_ω	The realization probability of scenario ω, where $\sum_\omega \eta_\omega = 1$
A_i^κ	Rooftop surface available at site i in region κ (m^2)
H_i^κ	Average hourly electricity consumption for space conditioning at site i in region κ (kWh)
ι_i^κ	Rooftop radiation potential of site i in region κ
Stochastic Parameters	
L_ω^κ	Total number of peak sunlight hours available in region κ under scenario ω over the planning horizon
λ_ω^κ	Total number of cooling degree-hours in region κ under scenario ω over the planning horizon
τ_ω^κ	Total number of heating degree-hours in region κ under scenario ω over the planning horizon

any installation, regardless of the size of the PV system, whereas the others are functions of the size of the system. For instance, the workforce cost consists of a fixed cost for engineering design, permit, and contract fees, plus a variable labor cost to install the system. Similarly, the PV system cost consists of a fixed cost for DC-AC power inverter and wiring, plus a variable cost for PV modules and mounting device that is a function of the PV system size. In the following, we first calculate the fixed and variable costs of the workforce. Next, we estimate the fixed and variable costs of the PV system components. We then use these values to estimate PV system fixed cost, F, and PV system variable cost in our region of interest, V^κ.

According to a 2015 report by the National Renewable Energy Laboratory (NREL) [27], installing a 5 kW PV system with a size of 37.5 m^2 (400 ft^2) on a residential rooftop costs $7,950, which includes the one-time engineering design, permit, and contract fees, plus the labor costs. In contrast, the cost of installing a commercial system of size 743.2 m^2 (8,000 ft^2) equals $92,132, including the one-time fees and labor costs. We assume the labor costs for installing the PV system increase linearly in the system size, and the one-time fees are equivalent. Let $\mathbb{W}$ denote the total workforce cost needed to install PV system and recall that k_i^κ denotes the area of PV panel installed at site $i \in I^\kappa$. Hence, using linear regression, we obtain $\mathbb{W} = 3500 + 120k_i^\kappa$. Consequently, we use the intercept of $3,500 and the slope of $120 per m^2 as the fixed and variable costs of workforce required for installing a PV system.

Connecting the PV system to the grid requires inverters to convert the direct current (DC) from PV panels into alternating current (AC). These inverters generally cost between $1,000 and $5,000 based on their capacity and quality [116,127], with relatively limited additional cost for wiring. In this study, we consider the average cost of $3,500 for the fixed cost of PV system components, which depending on the brand, is sufficient enough for purchasing inverters with a size of 3,000 W to 12,000W [127]. Hence, the PV system fixed cost, F, equals to $7,000, which consists of the fixed part of total workforce cost, i.e., $3,500, plus the inverter and wiring costs, i.e., $3,500.

As of 2017, PV modules cost between $0.85 and $1.5 per W. That is, for a panel with the size of 1 m^2 and 150W–250W output on top efficiency, the module cost ranges from $128 to $375, while the mounting device (frame) costs an additional $60 per m^2. Therefore, the PV system variable cost, V^κ, for the City of Knoxville, including the variable part of workforce cost, i.e., $120 per m^2, plus module and mounting device cost, ranges between $310 and $560 per m^2.

PV panel output, Q. Commonly available PV panels have an efficiency ranging from 13.5% to 20% [27]. Therefore, the real output of 1 m^2 panel during an hour of peak sunlight ranges from 135W–200W.

Total maintenance cost per m^2 PV panel installed in region κ, $\mathbb{C}^\kappa$. PV panels are made of tempered glass, making them able to withstand harsh weather conditions. Moreover, PV panels have no moving parts, except for panels with tracking mounts, making them very reliable and able to continue operation with minimal maintenance [18]. Most PV panel manufacturers guarantee their products for 20 to 25 years [126]. Therefore, if PV panels cease working, the PV panel companies will fix the issue at no cost. However, in order to utilize PV panels on their full potential, the surface of PV panels should be cleaned throughout their lifespan, which imposes an annual cleaning cost of $0.25 to $1.5 per panel [126], or equivalently $0.15 to $0.92 per m^2 of panel [48]. Note that these costs do not consider the positive impact of GRs on reducing air borne pollutants and dust in GR integrated PV panels [61].

Please cite this article as: M. Ramshani, A. Khojandi and X. Li et al., Optimal planning of the joint placement of Photovoltaic panels and green roofs under climate change uncertainty, Omega, https://doi.org/10.1016/j.omega.2018.10.016

Recall that in this study we use two planning horizon lengths, i.e., $T = 10$ and $T = 20$ years. Hence, assuming that the current estimated maintenance costs of \$0.15 to \$0.92 per m^2 of panel increase with inflation, we consider the total maintenance $\mathbb{C}^\kappa$, incurring in the beginning of the planning horizon, to range between \$1.5 and \$9.2 when $T = 10$ years and between \$3 and \$18.4 when $T = 20$ years.

Average hourly electricity consumption for space conditioning at site i in region κ, H_i^κ. Generally speaking, electricity consumption increases in building size [41]. We use the data available from a 2009 survey by the EIA [41] to characterize the relationship between the average hourly energy consumption for space conditioning and building size. Note that we consider a residential level of energy consumption for all the candidate sites in this study. The data suggests a strong linear relationship between the energy consumption and the building size, where it ranges between 25 m^2 and 400m^2. Recall that A_i^κ denotes the available rooftop surface at candidate site *i*. We assume that the total size of each building is equal to its available rooftop surface, and each candidate site corresponds to a single unit. Hence, the relationship can be best approximated as

$$H_i^\kappa = 0.508 + 0.004A_i^\kappa. \tag{10}$$

(For further details about the data and model, please refer to Appendix A.)

Cost per m^2 for installing GR in region κ, P^κ. GRs are typically classified into three main types, namely, extensive, semi-intensive, and intensive, mainly based on their types of vegetation and properties, such as weight, use, and maintenance [72]. In this study, consistent with the existing literature that focuses on energy saving aspect of GRs, we only consider extensive GR, which is the least expensive and most resilient type of GR [29,36,102]. According to the U.S. General Services Administration (GSA), the cost per m^2 of extensive GR is approximately \$12 [64] which includes the drainage layer cost as well as labor cost. Consistent with published reports, we do not consider setup costs for GRs [64].

Price per kWh sold to the grid, and cost per kWh purchased from the grid, γ and μ, respectively. Selling excess electricity generated to the grid and being paid in return [51], known as feed-in tariffs, or more specifically export tariffs [51], is not generally offered in the U.S., except in a limited number of states [47]. However, net metering, which allows for sending the extra electricity generated to the grid at normal retail value and receiving credit for it, is supported by most utility providers [112]. Therefore, consistent with these methods, we consider the same value for the electricity sold to and purchased from the grid as we assume the excess electricity that is sent to the grid can be credited and hence, used by any of the candidate sites. According to [38], as of 2017, each kWh of electricity purchased from the grid costs approximately 10.3 cents. Hence, we set μ and γ equal to 10.3 cents.

Percentage energy saving in cooling degree-hours due to GR installation, α, and percentage energy saving in heating degree-hours due to GR installation, β. The percentage of energy saving in cooling degree-hours achieved due to the installation of GRs differs across various studies, ranging from 10% to 16.7% [7,29,36,53,101,118,135]. While almost all studies agree on the fact that using GRs results in savings in cooling degree-hours, there is a lack of consensus on the impact of GRs in heating degree-hours. Indeed, a few empirical studies report that using GRs contribute to energy loss in heating degree-hours while others suggest that it results in energy savings. For instance, a recent, long-term study reports that GRs increase the required amount of energy to heat the space to a comfortable level (i.e., 22 °C in this study) in heating degree-hours by 6.2% [29]. Consistently, another study performed in different climates throughout Europe reports up to 1% GR-related energy loss in cold seasons in certain climates [7]. In contrast, two empirical studies suggest that the energy savings from GR in heating degree-hours is negligible and can be ignored [53,118]. However, there exists another group of studies that report reductions of 4% to 10% in energy savings as a result of GRs in heating degree-hours [7,36,101,135]. Therefore, in this study, we let α and β assume a wide range of values to capture the different, and sometimes contradicting, estimates reported in the literature. Specifically, we let α range from 10% to 20% and β range from −10% to 10%.

Percentage efficiency increase in the output of PV panels due to integration with GRs, θ. As the results from the previous studies show, integrating PV panels with GRs results in a higher panel efficiency, mainly due to the cooling effect of GRs. However, these studies report a relatively wide range of values for the percentage efficiency increase, i.e., from 3.33% to 8% [24,71].

Percentage change in energy consumed for space conditioning over the planning horizon, δ. In general, changes in human behavior with respect to energy consumption is not always easily quantifiable and can be impacted by various technological, sociological, climatic, and economic factors [66,69]. Over the past few decades, the level of energy consumption for space conditioning in the U.S. residential sector has experienced a steady decline, decreasing from 58% of overall energy consumption per household in 1993, to 48% in 2009 [42]. The projections for the energy consumption for space conditioning, on the other hand, are mixed [43,69]. Published studies report various degrees of increase/decrease in the level of energy consumption for space heating and cooling [4,13,70,87,88,104–107,111]. For instance, Scott et al. [111] project the decrease of 24% in the level of energy consumption for space heating and the increase of 39% in the level of energy consumption for space cooling by year 2020. In other studies, Huang [70] and Amato et al. [4] project the decrease of as much as 33% and 13% in the level of energy consumption for space heating, and the increase of as much as 158% and 40% for space cooling by years 2080 and 2030, respectively. Note that according to EIA [41], only a quarter of the total energy consumed for space conditioning in the U.S. residential sector is used for space cooling, while the remaining three quarters is used for space heating. Hence, in this study to capture a wide array of variability, we use a weighted average of the reported values for space heating and cooling, and consequently, account for up to 60% change in total energy consumption for space conditioning.

Initial budget available for investment, B. The net budget for 2017–2018 for the City of Knoxville is equal to \$378.8 million. The City dedicates a fraction of the budget to various long-term urban development projects. For instance, in the 2017–2018 budget, \$17.8 million is dedicated to the conversion of approximately 300,000 street lights across the City to the LED technology, for which the payback period is anticipated to be less than a decade [120]. Consistent with the budget allocated to this project and other investments in green technologies, in our case study, we set the initial budget available for investment, *B*, equal to \$20 million.

Table 2 summarizes the parameters that are calibrated from the literature and considered in our numerical studies. The table presents the ranges of values obtained from the literature. In our numerical studies, however, we capture a range slightly larger than the reported values to account for additional uncertainty and possible parameter estimation errors. We conduct our numerical studies at the discrete levels provided in the table.

3.2. Parameters estimated from data

To estimate the remaining parameters, we use a few datasets including climate projections and solar insolation provided by UDI [122] and CCSI [20].

Total number of cooling degree-hours, λ_ω^κ, and heating degree-hours, τ_ω^κ, in region κ under scenario ω over the planning horizon.

Please cite this article as: M. Ramshani, A. Khojandi and X. Li et al., Optimal planning of the joint placement of Photovoltaic panels and green roofs under climate change uncertainty, Omega, https://doi.org/10.1016/j.omega.2018.10.016

Table 2
Parameter values estimated from the literature and industry reports.

Parameter	Ranges	Levels	Sources
PV system variable cost, V^{κ} (USD)	[210,435]	100, 200, 400, 600	[27]
Annual maintenance cost per m^2 PV panel installed in region κ, $\frac{\mathbb{C}^{\kappa}}{T}$ (USD)	[0.15,0.92]	0.15, 0.62, 0.92	[18,126]
PV panel output, Q (W)	[135,200]	100, 200	[27,116]
Percentage energy saving in cooling degree-hours due to GR installation, α	[10%, 16.7%]	10%, 20%	[7,29,36,53,101,118,135]
Percentage energy saving in heating degree-hours due to GR installation, β	[−6.1%, 10%]	−10%, 10%	[7,29,36,53,101,118,135]
Percentage efficiency increase in the output of PV panels due to integration with GRs, θ	[3.33%, 8%]	2.5%, 10%	[24,71]
Percentage change in energy consumed for space conditioning over the planning horizon, δ	[−60%, 60%]	−60%, −40%, −20%,0%, 20%, 40%, 60%	[4,13,42,43,70,87,88,104–107,111]

Table 3
Ten coupled general circulation models (CGCMs) generated at Oak Ridge National Laboratory's Climate Change Science Institute [20] using high-performance computing resources, including Titan, America's fastest supercomputer [20].

Model	Institute of development
Japanese Meteorological Research Institute Coupled Global Climate Model (MRI-CGCM3)	Meteorological Research Institute of the Japan Meteorological Agency [75]
Max-Planck-Institute Earth System Model Mixed Resolution (MPI-ESM-MR)	Max Planck Institute for Meteorology [92]
Geophysical Fluid Dynamics Laboratory Earth System Model (GFDL-ESM2M)	Geophysical Fluid Dynamics Laboratory [100]
The Australian Community Climate and Earth System Simulator (ACCESS)	Commonwealth Scientific and Industrial Research Organization [33]
The NCAR's Community Climate System Model (CCSM4)	Climate and Global Dynamics Laboratory at the National Center for Atmospheric Research [93]
The Institute Pierre Simon Laplace Climate Model (IPSL-CM5A)	Institute Pierre Simon Laplace [74]
The Beijing Climate Center Climate System Model (BCC-CSM)	Beijing Climate Center, China Meteorological Administration [12]
Norwegian Earth System Model (NorESM1-M)	Multi-institutional, Coordinated Climate Research in Norway [37]
The Centro Euro-Mediterraneo sui Cambiamenti Climatici Climate Model (CMCC-CM)	Euro-Mediterranean Center on Climate Change [28]
Flexible Global Ocean Atmosphere Land System (FGOALS)	Institute of Atmospheric Physics, Chinese Academy of Sciences, State Key Laboratory of Numerical Modeling for Atmospheric Sciences and Geophysical Fluid Dynamics [83]

The climate system evolves as a result of slow changes in boundary conditions, physical parameters, ocean and sea ice, etc. [73]. General circulation models (GCMs) are climate models which exploit the general circulation mathematical model of a planetary atmosphere (atmospheric GCMs) or ocean (oceanic GCMs) to numerically simulate and project changes in Earth's climate system. Coupled GCMs (CGCMs) consist of models that combine atmospheric GCM (AGCM) with oceanic GCM (OGCM) into interactive ocean-atmosphere models [134]. In this study, we use the climate projections from ten CGCMs as listed in Table 3. The available projections consist of daily precipitation as well as minimum and maximum temperatures for 1 km^2 and 4 km^2 grids for the City of Knoxville from January 2011 through December 2050. In this study, we use the data for two planning horizons of length $T = 10$ years and $T = 20$ years, starting from January 2011. In order to reduce the computational effort, we use each climate projection as a scenario in our model, after averaging the daily projections for all grids spanning the City of Knoxville. We examine the impact of using the exact projections for each grid on the results in Section 4.3.

Note that the ten CGCMs are based on similar empirical or theoretical assumptions, hence they are somewhat correlated [76]. However, as discussed in Section 1, the projected daily temperatures and precipitation values vary across the ten CGCMs. Table 4 presents the maximum, average and the range of standard deviation for daily pairwise comparisons across the ten projections over the given planning horizon. As seen in Table 4, the average value of the pairwise differences for daily maximum and minimum temperatures for both $T = 10$ years and $T = 20$ years are on the order of 5 degrees Celsius, which highlight the existing variations in the projected values. (For detailed plots on daily/monthly/yearly average temperatures for the City of Knoxville, Tennessee for the ten different climate projections, please see Appendix B.)

As discussed, the data generated by CGCMs are on a daily basis. However, to accurately calibrate the model formulated in Section 2, we require hourly data. Hence, we use the widely accepted cosine function to disaggregate the temperature data into hourly predictions [59], i.e.,

$$Y_t = a\cos\left(\frac{\pi(t+b)}{12}\right) + c + \epsilon. \tag{11}$$

Using this function requires daily minimum and maximum temperatures, and the time of the day during which these extreme temperatures occur. Hence, to estimate these data points, we use the hourly historical data from 2010 to 2012 provided by McGhee Tyson Airport weather station in Knoxville [32], to obtain the time at which the daily minimum and maximum temperatures were previously observed. As shown in Fig. 3a, the daily minimum and maximum temperatures occur at different times during the day dependent on the month of the year. For instance, in the month of May, the daily minimum and maximum temperatures on average occur at 7 A.M. and 4 P.M., respectively, while in January, the daily minimum and the maximum temperatures on average occur at 9 A.M. and 5 P.M., respectively. Fig. 3b shows the hourly temperatures for ACCESS CGCM obtained from Eq. (11) and calibrated with the data presented in Fig. 3a. The same approach is used to obtain the hourly temperatures from the remaining nine CGCMs.

In order to estimate the total number of cooling and heating degree-hours during a given day, we need cut-off values to guide when cooling and heating are required. Recommended comfort human temperatures are often reported as 20 – 23.3 °C in winter and

Please cite this article as: M. Ramshani, A. Khojandi and X. Li et al., Optimal planning of the joint placement of Photovoltaic panels and green roofs under climate change uncertainty, Omega, https://doi.org/10.1016/j.omega.2018.10.016

Table 4
Maximum, average and the standard deviation range for daily pairwise comparisons across the projections from ten CGCMs, presented in Table 3, over two planning horizons of length $T = 10$ years and $T = 20$ years, starting from January 2011.

Parameter	T=10			T=20		
	Maximum	Average	Standard deviation range	Maximum	Average	Standard deviation range
Daily maximum temperature (°C)	30.63	4.71	[0.89,7.95]	31.41	4.72	[0.79,7.95]
Daily minimum temperature (°C)	41.58	4.82	[0.47,11.13]	41.58	4.79	[0.47,11.22]
Daily precipitation (mm)	105.26	5.40	[0.02,38.88]	105.26	5.45	[0.02,38.88]

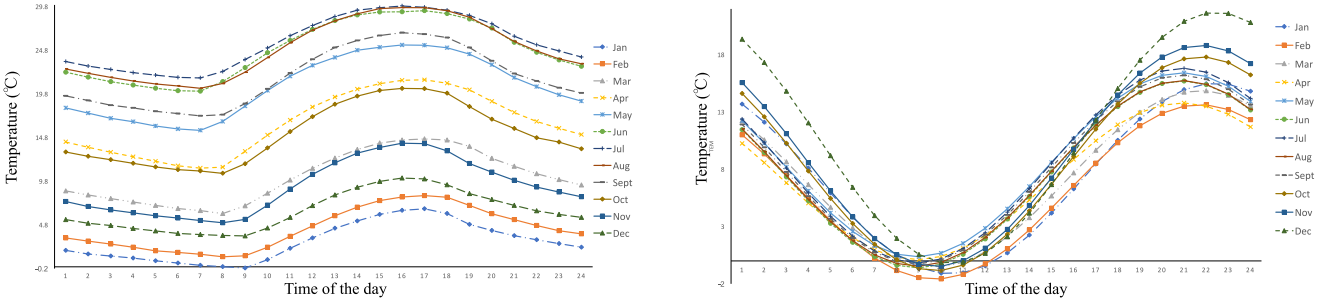

(a) The hourly temperatures in a day, averaged across month of the year from 2010 to 2012 based on the historical data (CRONOS, 2017).

(b) The ACCESS CGCM projected hourly temperatures in a day, averaged across month of the year from 2011 to 2021, obtained using Equation (11).

Fig. 3. Example hourly temperature values for the City of Knoxville.

22.8 to 25.6 °C in summer [19]. A 2009 survey conducted by the EIA [43] shows that in the U.S., residential households usually use space conditioning for heating and cooling when the outdoor temperature ranges between 14.4 and 17.8 °C, and 17.8 and 19.4 °C, respectively. In this study, consistent with the recent published works, we set the cut-off values for heating and cooling degree-hours to 22 and 18 °C, respectively [29,35].

Total number of peak sunlight hours available in region κ under scenario ω over the planning horizon, L^{κ}_{ω}. Our datasets report projected temperature and precipitation, but do not include the daily *peak* sunlight hours. Also note that the number of daily peak sunlight hours is different from the readily available number of daily sunlight hours [114]. Hence, we use the amount of daily precipitation to estimate the total number of peak sunlight hours available, L^{κ}_{ω}. Specifically, we assume that any day with a precipitation greater than 10mm is a cloudy day, and hence no peak sunlight hour is considered for such days. We obtain the estimate of 10mm by comparing the results for the years 2011 and 2012 with the annual average peak sunlight hours [34].

Rooftop radiation potential, ι^{κ}_{i}, rooftop surface available, A^{κ}_{i}, at site i in region κ, and total energy requirement for space conditioning in region κ over the planning horizon, R^{κ}. To obtain rooftop radiation potential, we use the solar insolation dataset provided by UDI [122] and CCSI [20]. This dataset includes the information about the rooftop size and solar insolation for 209,183 buildings in the City of Knoxville for the year 2003. The model that produces the data uses GIS and high-resolution Light Detection And Ranging (LiDAR) data to generate solar radiation intensity values for each building [79]. This high spatial and temporal resolution dataset is depicted in Fig. 4. As seen in Fig. 4, large rooftops generally have high solar insolation values mainly due to their flat surface and unobstructed access to the sunlight.

To estimate the values of ι^{κ}_{i}, we first obtain the per m^2 solar insolation values by dividing the solar insolation value of each rooftop by the size of the rooftop (in m^2). We then rescale them to range between 0 and 1.

NREL [56] defines three categories for building sizes, i.e., small (with rooftop sizes less than 185 m^2), medium (with rooftop sizes between 185 m^2 and 2,500m^2), and large (with rooftop sizes larger than 2,500m^2). Figs. 5a and b respectively show the distribution of rooftop sizes and solar insolation values for the 209,183 buildings in the City of Knoxville. As seen in Fig. 5b, in general, the larger the building, the larger the solar insolation value.

Recall that in Section 3.1, we assume that the total size of each building is equal to its available rooftop surface, and each candidate site corresponds to a single unit. Accordingly, Eq. (10) approximates the relationship between the available rooftop surface at a given candidate site and the corresponding average hourly electricity consumption for space conditioning at that site. Hence, based on the data provided by Kodysh et al. [79], we estimate the total energy requirement for space conditioning in the City of Knoxville to be approximately equal to 6.4 million GWh and 12.8 million GWh for $T = 10$ and $T = 20$, respectively.

The realization probability of scenario ω, η_{ω}. In this study we use the climate projections discussed earlier in this section as our scenarios. The parameter η_{ω} gives the likelihood that a scenario is realized. As discussed, climate projections can be correlated [76]. However, due to the lack of information about the exact development process of the CGCMs, here we assume that all scenarios are equally probable, i.e., $\eta_{\omega} = 0.1\ \forall \omega \in \Omega$.

4. Computational study

In this section, we provide extensive numerical results. First, we discuss the solution approach and introduce additional metrics in Section 4.1. Next, in Section 4.2 we provide a case study and discuss the results. Next, in Sections 4.3 and 4.4, we conduct extensive sensitivity and robustness analyses on model parameters, respectively, and provide insights. Finally, in Section 4.5 we discuss the environmental implications of the optimal solutions obtained in the case study.

4.1. Solution Approach and Additional Metrics

We use the L-shaped decomposition algorithm [124] to efficiently solve the problem. In order to implement this method, we

Please cite this article as: M. Ramshani, A. Khojandi and X. Li et al., Optimal planning of the joint placement of Photovoltaic panels and green roofs under climate change uncertainty, Omega, https://doi.org/10.1016/j.omega.2018.10.016

Fig. 4. Visual-SOLAR radiation map for the City of Knoxville, Tennessee [79].

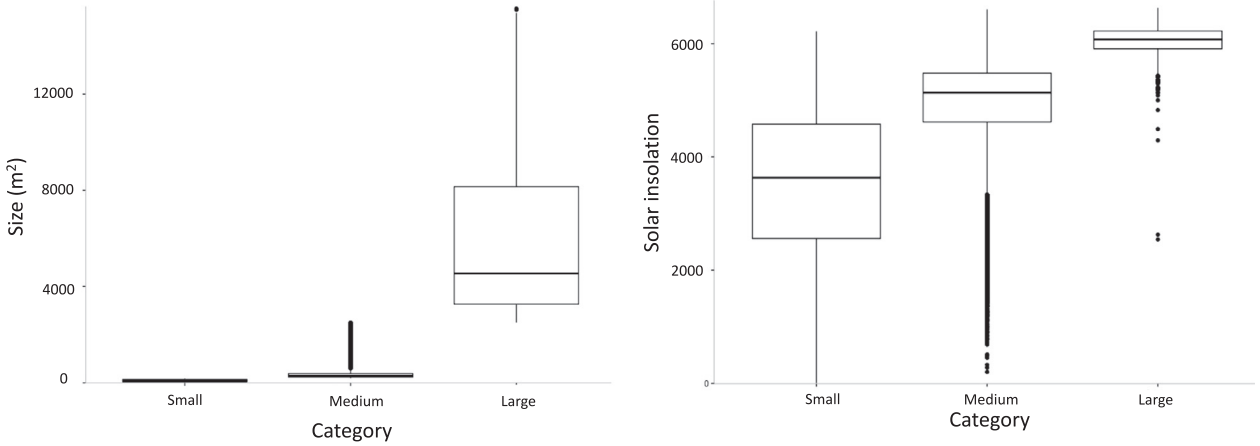

(a) Rooftop surface. (b) Solar insolation.

Fig. 5. Rooftop size and solar insolation for the 209,183 buildings in the City of Knoxville, stratified across rooftop size category.

Table 5
The parameter values in the three cases considered in the case study for the City of Knoxville.

Case study	PV panel output, Q (kW)	PV system variable cost, V (USD)	Percentage energy saving in cooling degree- hours by GRs, α	Percentage energy saving in heating degree- hours by GRs, β	Percentage efficiency increase in PV panel output, θ
Case 1	0.15	400	10%	0.0%	5%
Case 2	0.2	200	10%	0.0%	5%
Case 3	0.2	200	10%	0.0%	$\theta_t = 0.0013\mathbb{T}_t + 0.091$

linearize Eq. (6). To remove the non-linearity caused by $k_i^\kappa y_i^\kappa$, we employ the big M method [62]. We add two new continuous variables $\zeta_i^{1\kappa}$ and $\zeta_i^{2\kappa}$ to the model such that

$$\zeta_i^{1\kappa} + \zeta_i^{2\kappa} = k_i^\kappa, \quad \zeta_i^{1\kappa} \le M y_i^\kappa, \quad \zeta_i^{2\kappa} \le M\left(1 - y_i^\kappa\right) \quad \forall i, \kappa, \quad (12)$$

where M is a sufficiently large number. We add the set of constraints in Eq. (12) to the model and replace Eq. (6) with the following set of constraints:

$$e_{i\omega}^\kappa = QL_\omega^\kappa k_i^\kappa \iota_i^\kappa + QL_\omega^\kappa \iota_i^\kappa \zeta_i^{1\kappa}\theta \qquad \forall i, \omega, \kappa. \quad (13)$$

In the following we introduce two new metrics. These metrics are used to facilitate the comparison of the results.

Return on investment, ROI. Recall that our objective is to maximize the overall profit from energy generated and saved. However,

Please cite this article as: M. Ramshani, A. Khojandi and X. Li et al., Optimal planning of the joint placement of Photovoltaic panels and green roofs under climate change uncertainty, Omega, https://doi.org/10.1016/j.omega.2018.10.016

Table 6
Optimal solution for an initial budget of $20 million available for investment over two planning horizons of length $T = 10$ years and $T = 20$ years for the cases presented in Table 5.

	$T = 10$						$T = 20$					
	Stand-alone PV (m^2)	Stand-alone GR (m^2)	PV+GR (m^2)	Budget spent ($)	SI	ROI	Stand-alone PV (m^2)	Stand-alone GR (m^2)	PV+GR (m^2)	Budget spent ($)	SI	ROI
Case 1	0	999	0	11,988	0.0033%	75.82%	0	21,969	0	263,628	0.0283%	37.97%
Case 2	0	999	0	11,988	0.0033%	75.82%	99,612	2,295	0	20,000,000	2.8724%	84.60%
Case 3	0	999	0	11,988	0.0033%	75.82%	0	4,735	93,930	20,000,000	2.8893%	87.72%

to more easily compare the efficiency of the prescribed investment options, we introduce this new metric. Specifically, return on investment is calculated by dividing the net profit by the cost of investment multiplied by 100, i.e.,

$$\text{ROI} = \frac{\sum_i \sum_\kappa -\left(Fx_i^\kappa + k_i^\kappa V^\kappa + A_i^\kappa P^\kappa y_i^\kappa\right) + \sum_\omega \sum_i \sum_\kappa \eta_\omega \left(e_{i\omega}^\kappa + s_{i\omega}^\kappa\right)}{\sum_i \sum_\kappa \left(Fx_i^\kappa + k_i^\kappa V^\kappa + A_i^\kappa P^\kappa y_i^\kappa\right)} \times 100. \tag{14}$$

Sustainability index, SI. As discussed in Section 1, one of the major intangible, non-financial benefits associated with using PV panels and GRs is reducing the reliance on fossil fuels. This metric quantifies the percentage of the requisite energy that is saved or generated by using GRs and/or PV panels under the optimal solution, i.e.,

$$\text{SI} = \frac{\sum_\omega \sum_i \sum_\kappa \eta_\omega (e_{i\omega}^\kappa + s_{i\omega}^\kappa)}{\sum_\kappa R^\kappa} \times 100. \tag{15}$$

Although our objective is not to maximize SI, such metric can help policy makers to compare intangible benefits of the provided solutions.

4.2. Case study

In this section, we present the results for a case study for the City of Knoxville, Tennessee. Specifically, we examine a set of 209,183 buildings, as candidate sites in one region, given an initial investment budget of $20 million.

As discussed in the introduction, we take the perspective of a regional governing body throughout this paper. Nonetheless, the model is versatile and can be easily modified and calibrated to study the problem from other perspectives (e.g., utility companies).

Note that an average residential building in the southern U.S. built by 2010 is of size 220m^2 [21] and has 1.5 floors [22]. In this study, to capture the energy savings of GRs which typically only provide energy savings for the top floor unit(s), we assume all buildings are single units.

In order to capture the effects of current prices and efficiency of the PV panels, we consider three cases. In this section, we set $\delta = 0$. We later conduct sensitivity analysis on the impact of parameter δ on the solutions. In these cases, we use the values estimated form the literature and summarized in Table 2. Specifically, in all three cases, we set the percentage energy saving in cooling and heating degree-hours by GRs, i.e., α and β, respectively, equal to 10% and 0%. In Case 1, we consider the price and efficiency of current commercially available panels. That is, we set the PV panel output, Q, and the PV system variable cost in the City of Knoxville, V^κ, equal to 0.15 and 400, respectively. As discussed in Section 1 the cost of PV panels is on the decline while their efficiency is increasing. Hence, Case 2 considers efficient PV panels with lower than average cost to capture a likely upcoming scenario. In both Cases 1 and 2 we set the percentage efficiency increase in the output of PV panels due to integration with GRs, θ, equal to 5%. Note that θ is directly related to the ability of GRs to reduce their surrounding environment temperature. In Case 3, we use the range reported in Table 2 to approximate a linear relationship between hourly percentage efficiency increase in the output of PV panels due to integration with GRs and hourly temperature. In this case, unlike Cases 1 and 2 in which we consider a fixed value for θ regardless of the outside temperature, we incorporate the effect of the outside temperature in the GR-provided efficiency increase of PV panels. Let θ_t denote hourly percentage efficiency increase in the output of PV panels due to integration with GRs and $\mathbb{T}_t$ denote the hourly temperature. From the linear regression we obtain $\theta_t = 0.0013\mathbb{T}_t + 0.091$. Applying this function to the climate projections results in θ_t values that range from 0.064 to 0.14,

Table 7
Area covered by stand-alone GRs, stand-alone PV panels, and GR integrated PV panels under different values for PV panel output, PV system variable cost, percentage energy saving in cooling and heating degree-hours due to GR installation, and percentage efficiency increase in the output of PV panels due to integration with GRs for an initial budget of $20 million available over two planning horizons of length $T = 10$ years and $T = 20$ years.

					$T = 10$					$T = 20$				
PV panel output, Q (kW)	PV system variable cost, V^{κ} (USD)	Percentage energy saving in cooling degree-hours by GRs, α	Percentage energy saving in heating degree-hours by GRs, β	Percentage efficiency increase in PV panel output, θ	Stand-alone PV (m^2)	Stand-alone GR (m^2)	PV+GR (m^2)	SI	ROI	Stand-alone PV (m^2)	Stand-alone GR (m^2)	PV+GR (m^2)	SI	ROI
10%	100	10%	-10%	2.5%	0	0	0	0.000%	0.00%	199,400	0	0	1.283%	82.43%
				10%	0	885	178,030	1.965%	63.13%	0	885	178,030	3.508%	225.45%
			10%	2.5%	0	76,875	0	0.056%	38.76%	187,087	103,443	0	1.356%	87.12%
				10%	0	14,344	176,410	2.031%	65.26%	0	14,344	176,410	3.574%	229.68%
		20%	-10%	2.5%	0	0	0	0.000%	0.00%	199,396	31	0	1.283%	82.43%
				10%	0	885	178,030	1.979%	63.59%	0	885	178,030	3.523%	226.39%
			10%	2.5%	0	192,650	0	0.155%	43.22%	169,430	250,580	0	1.480%	95.14%
				10%	0	34,058	174,386	2.074%	66.65%	0	34,074	174,385	3.618%	232.52%
	200	10%	-10%	2.5%	0	0	0	0.000%	0.00%	0	0	0	0.000%	0.00%
				10%	0	0	0	0.000%	0.00%	0	2302	94,068	1.145%	73.62%
			10%	2.5%	0	76,875	0	0.056%	38.76%	0	589,660	0	0.270%	49.03%
				10%	0	76,875	0	0.056%	38.76%	0	104,608	88,277	1.251%	80.43%
		20%	-10%	2.5%	0	0	0	0.000%	0.00%	0	137	0	0.000%	23.42%
				10%	0	0	0	0.000%	0.00%	0	2335	94,066	1.153%	74.12%
			10%	2.5%	0	192,650	0	0.155%	43.22%	0	1,166,725	0	0.641%	58.85%
				10%	0	192,650	0	0.155%	43.22%	0	251,691	79,999	1.394%	89.60%
	400	10%	-10%	2.5%	0	0	0	0.000%	0.00%	0	0	0	0.000%	0.00%
				10%	0	0	0	0.000%	0.00%	0	0	0	0.000%	0.00%
			10%	2.5%	0	76,875	0	0.056%	38.76%	0	589,660	0	0.270%	49.03%
				10%	0	76,875	0	0.056%	38.76%	0	589,660	0	0.270%	49.03%
		20%	-10%	2.5%	0	0	0	0.000%	0.00%	0	137	0	0.000%	23.42%
				10%	0	0	0	0.000%	0.00%	0	137	0	0.000%	23.42%
			10%	2.5%	0	192,650	0	0.155%	43.22%	0	1,166,725	0	0.641%	58.85%
				10%	0	192,650	0	0.155%	43.22%	0	1,166,725	0	0.641%	58.85%
	600	10%	-10%	2.5%	0	0	0	0.000%	0.00%	0	0	0	0.000%	0.00%
				10%	0	0	0	0.000%	0.00%	0	0	0	0.000%	0.00%
			10%	2.5%	0	76,875	0	0.056%	38.76%	0	589,660	0	0.270%	49.03%
				10%	0	76,875	0	0.056%	38.76%	0	589,660	0	0.270%	49.03%
		20%	-10%	2.5%	0	0	0	0.000%	0.00%	0	137	0	0.000%	23.42%
				10%	0	0	0	0.000%	0.00%	0	137	0	0.000%	23.42%
			10%	2.5%	0	192,650	0	0.155%	43.22%	0	1,166,725	0	0.641%	58.85%
				10%	0	192,650	0	0.155%	43.22%	0	1,166,725	0	0.641%	58.85%

(*continued on next page*)

Please cite this article as: M. Ramshani, A. Khojandi and X. Li et al., Optimal planning of the joint placement of Photovoltaic panels and green roofs under climate change uncertainty, Omega, https://doi.org/10.1016/j.omega.2018.10.016

Table 7 (*continued*)

PV panel output, Q (kW)	PV system variable cost, V^{κ} (USD)	Percentage energy saving in cooling degree-hours by GRs, α	Percentage energy saving in heating degree-hours by GRs, β	Percentage efficiency increase in PV panel output, θ	$T = 10$					$T = 20$				
					Stand-alone PV (m^2)	Stand-alone GR (m^2)	PV+GR (m^2)	SI	ROI	Stand-alone PV (m^2)	Stand-alone GR (m^2)	PV+GR (m^2)	SI	ROI
20%	100	10%	-10%	2.5%	199,300	0	0	2.580%	82.91%	199,300	0	0	4.122%	264.89%
				10%	0	885	178,030	7.054%	226.66%	0	885	178,030	8.584%	551.67%
			10%	2.5%	198,435	8039	0	2.593%	83.33%	198,435	8039	0	4.135%	265.72%
				10%	0	1589	177,955	7.110%	228.47%	0	1589	177,955	8.640%	555.27%
		20%	-10%	2.5%	199,300	0	0	2.580%	82.91%	199,300	0	0	4.122%	264.89%
				10%	0	885	178,030	7.068%	227.12%	0	885	178,030	8.598%	552.61%
			10%	2.5%	196,007	28,274	0	2.615%	84.05%	196,007	28,274	0	4.158%	267.20%
				10%	0	3455	177,755	7.128%	229.05%	0	3455	177,755	8.658%	556.45%
	200	**10%**	**-10%**	**2.5%**	**0**	**0**	**0**	**0.000%**	**0.00%**	**99,750**	**0**	**0**	**1.315%**	**84.49%**
				10%	0	2302	94,068	2.311%	74.26%	0	2302	94,068	3.853%	247.65%
			10%	2.5%	0	76,875	0	0.056%	38.76%	93,643	103,443	0	1.386%	89.09%
				10%	0	10,824	93,585	2.351%	75.56%	0	10,824	93,585	3.893%	250.22%
		20%	-10%	2.5%	0	0	0	0.000%	0.00%	99,748	31	0	1.315%	84.49%
				10%	0	2302	94,068	2.319%	74.51%	0	2302	94,068	3.861%	248.16%
			10%	2.5%	0	192,650	0	0.155%	43.22%	84,815	250,580	0	1.508%	96.88%
				10%	0	39,001	91,849	2.381%	76.52%	0	39,001	91,849	3.924%	252.21%
	400	10%	-10%	2.5%	0	0	0	0.000%	0.00%	0	0	0	0.000%	0.00%
				10%	0	0	0	0.000%	0.00%	0	192	48,490	1.256%	80.74%
			10%	2.5%	0	76,875	0	0.056%	38.76%	0	589,660	0	0.270%	49.03%
				10%	0	76,875	0	0.056%	38.76%	0	106,739	45,386	1.340%	86.09%
		20%	-10%	2.5%	0	0	0	0.000%	0.00%	0	137	0	0.000%	23.42%
				10%	0	0	0	0.000%	0.00%	0	224	48,489	1.260%	80.99%
			10%	2.5%	0	192,650	0	0.155%	43.22%	0	1,166,725	0	0.641%	58.85%
				10%	0	192,650	0	0.155%	43.22%	0	251,111	41,181	1.470%	94.49%
	600	10%	-10%	2.5%	0	0	0	0.000%	0.00%	0	0	0	0.000%	0.00%
				10%	0	0	0	0.000%	0.00%	0	774	32,648	0.350%	22.49%
			10%	2.5%	0	76,875	0	0.056%	38.76%	0	589,660	0	0.270%	49.03%
				10%	0	76,875	0	0.056%	38.76%	0	330,878	26,176	0.527%	33.89%
		20%	-10%	2.5%	0	0	0	0.000%	0.00%	0	137	0	0.000%	23.42%
				10%	0	0	0	0.000%	0.00%	0	804	32,648	0.353%	22.66%
			10%	2.5%	0	192,650	0	0.155%	43.22%	0	1,166,725	0	0.641%	58.85%
				10%	0	192,650	0	0.155%	43.22%	0	703,127	18,877	0.788%	50.67%

Please cite this article as: M. Ramshani, A. Khojandi and X. Li et al., Optimal planning of the joint placement of Photovoltaic panels and green roofs under climate change uncertainty, Omega, https://doi.org/10.1016/j.omega.2018.10.016

Table 8
Area covered by stand-alone GRs, stand-alone PV panels, and GR integrated PV panels under different values of δ, for an initial budget of $20 million available over two planning horizons of length $T = 10$ years and $T = 20$ years for the cases presented in Table 5.

		$T = 10$						$T = 20$					
Case study	The rate of energy consumption, δ	Stand-alone PV (m^2)	Stand-alone GR (m^2)	PV+GR (m^2)	Budget spent ($)	SI	ROI	Stand-alone PV (m^2)	Stand-alone GR (m^2)	PV+GR (m^2)	Budget spent ($)	SI	ROI
Case 1	-60%	0	137	0	1,644	0.0009%	40.87%	0	629	0	7,548	0.0025%	69.98%
	-40%	0	389	0	4,668	0.0018%	49.60%	0	3,506	0	42,072	0.0077%	41.02%
	-20%	0	629	0	7,548	0.0025%	67.97%	0	8,039	0	96,468	0.0138%	46.60%
	20%	0	3,506	0	42,072	0.0076%	39.35%	0	45,121	0	541,452	0.0478%	36.14%
	40%	0	5,474	0	65,688	0.0104%	41.99%	0	76,875	0	922,500	0.0705%	37.43%
	60%	0	8,039	0	96,468	0.0136%	44.87%	0	116,127	0	1,393,524	0.0947%	39.74%
Case 2	-60%	0	137	0	1,644	0.0009%	40.87%	99,792	137	0	20,000,000	7.1776%	84.52%
	-40%	0	389	0	4,668	0.0018%	49.60%	99,777	389	0	20,000,000	4.7856%	84.54%
	-20%	0	629	0	7,548	0.0025%	67.97%	99,740	999	0	20,000,000	3.5899%	84.57%
	20%	0	3,506	0	42,072	0.0076%	39.35%	99,422	5,474	0	20,000,000	2.3949%	84.70%
	40%	0	5,474	0	65,688	0.0104%	41.99%	99,268	8,039	0	20,000,000	2.0544%	84.85%
	60%	0	8,039	0	96,468	0.0136%	44.87%	99,051	11,649	0	20,000,000	1.7997%	85.06%
Case 3	-60%	0	137	0	1,644	0.0009%	40.88%	0	2,447	94,060	20,000,000	7.2069%	88.59%
	-40%	0	389	0	4,668	0.0018%	49.60%	0	2,715	94,044	20,000,000	4.8064%	88.63%
	-20%	0	629	0	7,548	0.0025%	67.97%	0	2,969	94,030	20,000,000	3.6064%	85.33%
	20%	0	3,506	0	42,072	0.0076%	39.35%	0	6,019	93,857	20,000,000	2.4116%	87.87%
	40%	0	5,474	0	65,688	0.0104%	41.99%	0	10,824	93,585	20,000,000	2.0694%	86.89%
	60%	0	8,039	0	96,468	0.0136%	44.87%	0	14,650	93,369	20,000,000	1.8130%	87.18%

which are larger than θ values considered in both Case 1 and Case 2. Table 5 summarizes the three cases considered.

We use Gurobi Optimizer version 7.5 [65] on an iMac Pro-with an 8-core 3.2 GHz Intel Xeon W processor and 32GB of RAM to solve the model. The solution time for the three cases ranges between 422.2 s and 463.6 s. Appendix C provides further details on the solution time, number of variables, and number of constraints for the three cases.

Table 6 provides the optimal solutions for the three cases presented in Table 5. In all three cases, the total energy generated/saved is not enough to fully compensate the requisite energy needs of the City of Knoxville for space conditioning, either because of non-profitability of PV panels/GRs or the limited available budget for investment. Hence, in all these cases, the value of the objective function is negative. However, as seen in the table, ROIs are positive, suggesting that the income from the total energy generated/saved is higher than the budget spent.

First, note that when $T = 10$ only a small proportion of the available budget is spent under the optimal solution and only GRs are installed in all three cases. This is mainly due to the fact that when $T = 10$, the amount of electricity generated by PV panels is not nearly enough to cover their installation costs. In addition, because only GRs are installed in these three cases and the values for α and β are identical across the cases, the solutions and the metrics are also the same.

Similarly, when $T = 20$ in Case 1 only GRs are installed under the optimal solution and not all available budget is spent. However, in Cases 2 and 3, the optimal solution also prescribes to install PV systems and all available budget is allocated. Specifically, in Case 1, 21,969m^2 of stand-alone GRs are installed under the optimal solution. Considering the average residential building rooftop size of 145m^2 in the southern U.S. [21], this is enough to cover to approximately 152 average residential buildings. In Case 2, more than 99% of the available budget is allocated to installing 99,612m^2 of stand-alone PV panels, and the rest of the budget is allocated to installing 2,295 m^2 of stand-alone GRs, in total covering an approximately 703 average residential buildings. Note that in this case GRs are not integrated with PV panels; hence, they are mainly installed to provide energy savings. In Case 3, approximately 94% of the budget is allocated to installing PV panels, all of which GR integrated, and the rest is used for installing an additional 4,735 m^2 of stand-alone GRs. In total, under the optimal solution, these practices cover an approximately 680 average residential buildings. Recall that estimated percentage efficiency increase in the output of PV panels due to integration with GRs in Case 3 is overall higher than the two other cases. Hence, in Case 3 more budget is allocated to GRs compared to Case 2 and all panels are GR integrated to achieve a higher electricity output. Note that contrary to Case 2, in Case 3 GRs are mainly used to help improve the output of PV panels.

The model generally prescribes the stand-alone GRs to be installed on small rooftops. Recall that Eq. (10) presents the relationship between hourly energy consumption for space conditioning and building size. From Eq. (10), the magnitude of the intercept is much larger than that of the slope. Therefore, for instance, two small buildings would consume more energy than a large building that has a rooftop area equivalent to the total area of the two small rooftops. Note that the energy savings from GRs are a fraction of the total energy consumed by the buildings (based on α and β.) Therefore, because GRs do not have a set up cost, when it is optimal to install stand-alone GRs, the model typically prioritizes small rooftops to generate more profit through their energy savings.

In contrast, the model generally prescribes to install PV panels on large rooftops, partially due to the fact that installing PV systems has a fixed set-up cost. Additionally, as discussed in Section 3.2, buildings with large rooftops often have the highest radiation potential, ι_i^{κ}, as they are mostly flat and unlikely to

Please cite this article as: M. Ramshani, A. Khojandi and X. Li et al., Optimal planning of the joint placement of Photovoltaic panels and green roofs under climate change uncertainty, Omega, https://doi.org/10.1016/j.omega.2018.10.016

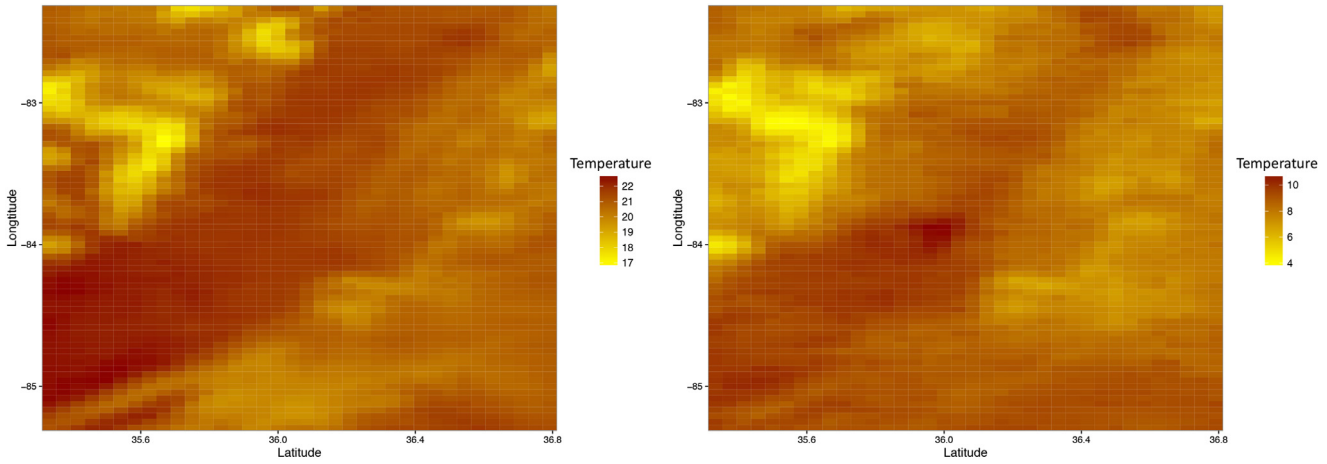

(a) Average daily maximum temperature. (b) Average daily minimum temperature.

Fig. 6. Heat map for average daily maximum and minimum temperatures over the year 2030 projected by the ACCESS CGCM across 4-km wide grids for the City of Knoxville.

be completely shaded by their surrounding buildings. Hence, the model prioritizes large rooftops for PV installation to minimize the cost while maximizing the electricity generation.

As shown in Table 6, for $T = 10$ years, Cases 1–3 result in the same ROI values as the corresponding solutions are identical. For $T = 20$ years, the solutions vary for the three cases and the highest ROI value is achieved in Case 3 in which the benefit of GRs are most accurately captured. The SI values in Table 6 are generally higher for $T = 20$ years compared to $T = 10$ years, as PV panels are installed for $T = 20$ years.

4.3. Sensitivity analysis

In this section, we conduct extensive sensitivity analysis to evaluate the impact of model parameters on the optimal solution. First, we conduct a sensitivity analysis on an array of parameters related to PV panels, GRs, and their interaction. Second, we examine the impact of possible changes in energy consumed for space conditioning over the planning horizon on optimal solutions. Next, we investigate the impact of incorporating maintenance cost directly into the model as a responsibility of the entity in charge of planning, e.g., the regional governing body. Lastly, we evaluate the impact of using the averages of the daily projections over all grids spanning the City of Knoxville, instead of the true projections for each grid, when calibrating the model, and provide recommendations.

Table 7 presents the results from the sensitivity analysis for different levels of PV system variable cost, V^{κ}, PV panel output, Q, percentage efficiency increase in the output of PV panels due to integration with GRs, θ, and percentage energy saving in cooling and heating degree-hours due to GR installation, α and β, respectively, as presented in Table 2. In general, when PV systems are expensive but have relatively low output, i.e., high V^{κ} values and low Q values, the optimal solution mainly depends on the energy savings from GRs. In this case, if the percentage energy saving in heating degree-hours due to GR installation, β, is low, no additional profit can be generated from installing GRs or PV panels. Hence, the model chooses to not spend any budget at all. When β is high, the model chooses to spend budget but only for stand-alone GRs, mainly to achieve energy savings, and hence maximize the profit. In this case, the total number of stand-alone GRs depends on and increases in the percentage energy saving in cooling degree-hours due to GR installation, α.

For cost-efficient PV systems, i.e., low V^{κ} values and high Q values, the optimal solution mainly depends on the percentage efficiency increase in the output of PV panels due to integration with GRs, θ. That is, when θ is low, the optimal solution is to install stand-alone PV panels. However, when θ is high, the model takes full advantage of the added efficiency and prescribes to install a large quantity of GR integrated PV panels, with the remaining budget spent on stand-alone GRs. In this case, the proportion of budget spent on stand-alone GRs increases in both α and β.

In general, the length of the planning horizon can significantly impact the optimal solution. For instance, as the highlighted row on Table 7 shows, for $T = 10$ years the optimal solution is to not spend any budget, whereas for $T = 20$ years the optimal solution is to allocate all of the budget to install stand-alone PV panels.

Additionally, ROI and SI values are generally higher for $T = 20$ years compared to $T = 10$ years. To eliminate the effect of different planning horizon lengths, we calculate the average annual ROI and SI values for $T = 10$ years and $T = 20$ years by dividing the values in the table by their planning horizon lengths. The results show that for $T = 20$ years the average annual ROI and SI values are at least as large as the average annual values for $T = 10$ years for any combination of parameters. This is mainly due to the higher number of peak sunlight hours and cooling degree-hours during the second decade of the 20-year planning horizon.

Overall, the results from Table 7 show that while the optimal solution of the model relies on the values of the key parameters, the length of the planning horizon, T, plays a significant role in the allocation of the initial investment. Moreover, Table 7 shows that both the percentage energy saving in cooling and heating degree-hours due to GR installation, α and β, and percentage efficiency increase in the output of PV panels due to integration with GRs, θ, can significantly affect the optimal solution. The values of α and β rely on several different factors, e.g., the type of green media or isolation layer installed, and vary significantly from one climate type to another. Hence, region-specific studies are needed to accurately estimate these parameters before large-scale implementation. In addition, to the best of our knowledge and despite the overwhelming evidence on the benefits of PV-GR integration, these benefits are not completely characterized in the literature. Hence, there is a need to further investigate and quantify this efficiency increase to better justify large-scale investments.

Table 8 presents the results of a sensitivity analysis with respect to percentage change in energy consumed for space conditioning over the planning horizon, δ, using its estimated values as presented in Table 2, for the three cases presented in Table 5. First, note that the optimal solutions presented in Table 8 are more or less consistent with those presented in Table 6, where $\delta = 0$. That

Please cite this article as: M. Ramshani, A. Khojandi and X. Li et al., Optimal planning of the joint placement of Photovoltaic panels and green roofs under climate change uncertainty, Omega, https://doi.org/10.1016/j.omega.2018.10.016

Table 9
Area covered by stand-alone GRs, stand-alone PV panels, and GR integrated PV panels under different values of $\mathbb{C}^{\kappa}$, for an initial budget of $20 million available over two planning horizons of length $T = 10$ years and $T = 20$ years for the cases presented in Table 5.

		$T = 10$						$T = 20$					
Case study	Annual per m^2 PV panel maintenance cost, $\frac{\mathbb{C}^{\kappa}}{T}$ ($)	Stand-alone PV (m^2)	Stand-alone GR (m^2)	PV+GR (m^2)	Budget spent ($)	SI	ROI	Stand-alone PV (m^2)	Stand-alone GR (m^2)	PV+GR (m^2)	Budget spent ($)	SI	ROI
Case 1	0.15	0	999	0	11,988	0.0033%	75.82%	0	21,969	0	263,628	0.0283%	37.97%
	0.62	0	999	0	11,988	0.0033%	75.82%	0	21,969	0	263,628	0.0283%	37.97%
	0.92	0	999	0	11,988	0.0033%	75.82%	0	21,969	0	263,628	0.0283%	37.97%
Case 2	0.15	0	999	0	11,988	0.0033%	75.82%	98,122	2295	0	20,000,000	2.8307%	81.93%
	0.62	0	999	0	11,988	0.0033%	75.82%	94,001	2295	0	20,000,000	2.7118%	74.28%
	0.92	0	999	0	11,988	0.0033%	75.82%	91,317	3506	0	20,000,000	2.6372%	69.49%
Case 3	0.15	0	999	0	11,988	0.0033%	75.82%	0	6140	92,525	20,000,000	2.8476%	84.96%
	0.62	0	999	0	11,988	0.0033%	75.82%	0	4018	88,876	20,000,000	2.7291%	77.13%
	0.92	0	999	0	11,988	0.0033%	75.82%	0	4362	86,470	20,000,000	2.6547%	72.41%

is, when $T = 10$, under the optimal solution, only a small proportion of the available budget is spent and only stand-alone GRs are installed. Also, when $T = 20$, in Case 1 only a limited number of stand-alone GRs are installed, whereas in Cases 2 and 3, the majority of the available budget is spent to place stand-alone PV panels and GR integrated PV panels, respectively, and the remaining budget is used for stand-alone GRs. In all three cases, the total area of installed GRs (i.e., stand-alone GRs and GR integrated PV panels) increases in δ, whereas the total area of installed PV panels (i.e., stand-alone PV panels and GR integrated PV panels) decreases in δ. Note that a larger δ means a higher amount of energy consumption over the planning horizon. Hence, when δ is large, GRs, which can save a fraction of the total energy consumed, provide additional benefits compared to PV panels. Therefore, as δ increases, the model allocates a larger portion of the budget to GRs.

It is interesting to note the extent to which the value of δ affects the decisions. For instance, when $T = 20$, the increase in δ drastically increases the total area of installed stand-alone GRs in Case 1, whereas this increase is more modest in Case 2 and especially in Case 3. This is mainly because in Case 1, not all of the budget is allocated. Also, only GRs are economically profitable. Hence, as δ increases, additional GRs are installed to provide further benefit. However, in Case 2, in which all of the budget is already allocated, for stand-alone GRs to be further prioritized over stand-alone PV panels, the energy savings achieved through their installation must be higher than the energy generated by PV panels. Therefore, the increase in δ only modestly increases the area of installed stand-alone GRs. In Case 3, in which again all of the budget is already allocated, PV panels installed enjoy an increase in the output as a result of integration with GRs. Therefore, compared to Case 2, stand-alone GRs face more resistance in being prioritized over GR integrated PV panels, hence a slower growth in the total area of installed stand-alone GRs in this case.

Moreover, for the cases in which all of the budget is spent under the optimal solution, i.e., in Cases 2 and 3 when $T = 20$, SI decreases, whereas ROI increases in δ. Recall that higher levels of δ leads to higher levels of profit through the installation of GRs. Therefore, given the same $20 million budget, the amount of savings increases in δ, resulting in higher profit and ROI. However, because the amount of increase in GR energy savings is smaller than that of energy consumption, SI decreases in δ.

Lastly, for the cases in which only a small proportion of the budget is spent on installing stand-alone GRs under the optimal solution, i.e., Cases 1–3 when $T = 10$ and Case 1 when $T = 20$, the amount of budget spent and SI both increase in δ. This is mainly because higher δ increases the achievable profit through the installation of GRs, making this practice a viable option for a larger number of candidate sites. As a result, a larger proportion of the budget is used to install a larger area of GRs across the candidate sites, leading to higher values of SI.

Table 9 presents the results when maintenance costs are directly incorporated into the model, using the estimated values as presented in Table 2, for the three cases presented in Table 5. First, note that for in all cases when $T = 10$ and in Case 1 when $T = 20$, the results in Table 9 remain the same as those obtained when maintenance costs are assumed to be the property owners' responsibility, presented in Table 6. This is because in these cases, it is not optimal to install PV panels even without incorporating their maintenance costs directly into the model and accounting for PV maintenance costs only makes them a more costly, and hence less favorable, option.

As seen in Table 9, for Cases 2 and 3 when $T = 20$, accounting for PV panel maintenance costs impacts the optimal solutions and negatively affects the ROI and SI metrics. In general, consistent with the intuition, the higher the PV maintenance cost, the more costly the PV panels and hence, the lower the total area of

Please cite this article as: M. Ramshani, A. Khojandi and X. Li et al., Optimal planning of the joint placement of Photovoltaic panels and green roofs under climate change uncertainty, Omega, https://doi.org/10.1016/j.omega.2018.10.016

PV panels installed. In particular, in Case 2, when the annual per m^2 PV maintenance cost increases from \$0.15 to \$0.62, stand-alone PV panels become more expensive and the portion of spent budget that is allocated to PV panels results in fewer square meters of PV panels. When the annual per m^2 PV maintenance cost increases further from \$0.62 to \$0.92, stand-alone PV panels become a less favorable option compared to stand-alone GRs and hence, more of the budget is spent on the latter and the total area of stand-alone PVs drops further. A similar trend is observed for Case 3, in which as the per m^2 PV maintenance cost increases, GR integrated PV panels become more expensive and consequently, the portion of spent budget that is allocated to PV panels results in fewer square meters of PV panels. However, in this case, GR integrated PV panels generally remain a favorable option despite the increase in their cost. Hence, as the annual per m^2 PV maintenance cost increases, a larger portion of the budget is allocated to GR integrated PV panels to mitigate the effect of their increased cost. Finally, the remaining portion of the budget that is not spent on installing GR integrated PV panels is allocated to install stand-alone GRs.

Finally, we investigate the impact of using the averages of the daily projections over all grids spanning the City of Knoxville, instead of the true projections for each grid, when calibrating the model. As discussed, the daily temperature projections are generated for grids of sizes 1 km^2 and 4 km^2. The daily maximum and minimum temperature projections of the 10 CGCMs show a variation across grids in the City of Knoxville. For instance, Figs. 6a and b depict the heat map of average daily maximum and minimum temperatures over the year 2030 projected by the ACCESS CGCM across 4-kilometer wide grids for the City of Knoxville. Other climate models show a similar pattern, indicating the variation in the hourly temperatures over different grids.

Here, we examine the impact of accounting for the exact projections provided for each grid through a grid-based calibration approach. Specifically, we calculate the total number of cooling and heating degree-hours for each 4 km^2 grid separately, assign each candidate site with the parameters of their corresponding grid, and then resolve the model. Table 10, which is analogous to Table 6, presents the optimal solution for two planning horizons of length $T = 10$ years and $T = 20$ years for the three cases presented in Table 5. As seen in the table, more GRs are installed under the grid-based calibration approach. For instance, in Case 1 for $T = 20$ years, the optimal solution prescribes to increase the total area of stand-alone GRs installed by 80%. This is due to the fact that most of the small and medium buildings in the City of Knoxville are located in the warmer grids and they are assigned a higher number of cooling degree-hours under the grid-based calibration approach. Hence, by installing more GRs the model can achieve more energy savings and consequently a higher profit. The increase in energy savings is also reflected in the SI values. The highest percentage of increase in SI values is equal to 2.22% for Case 1 when $T = 20$ years, which translates into 276.5 GWh of energy saved and generated through sustainable resources.

In general, the grid-based calibration approach provides more accurate representation of the problem at hand. However, the solution provided in Table 10 is relatively consistent with that of Table 6. Hence, considering that the data pre-processing for the grid-based calibration approach is much more computationally expensive, it may or may not be beneficial to use the grid-based calibration approach depending on the specific characteristics of the region of interest.

4.4. Robustness analysis

As discussed earlier, limited data is available for estimating some of the important model parameters. Hence, it is not unlikely that these parameters are wrongly estimated during implementa-

Table 10
Optimal solution for an initial budget of \$20 million available for investment over two planning horizons of length $T = 10$ years and $T = 20$ years for the cases presented in Table 5 under the grid-based calibration approach.

	$T = 10$						$T = 20$					
	Stand-alone PV (m^2)	Stand-alone GR (m^2)	PV+GR (m^2)	Budget spent	SI	ROI	Stand-alone PV (m^2)	Stand-alone GR (m^2)	PV+GR (m^2)	Budget spent	SI	ROI
Case 1	0	2813	0	33,756	0.0076%	43.98%	0	39,551	0	474,612	0.0505%	36.75%
Case 2	0	2813	0	33,756	0.0076%	43.98%	99,521	3818	0	20,000,000	2.8736%	84.68%
Case 3	0	2813	0	33,756	0.0076%	43.98%	0	5989	93,859	20,000,000	2.8941%	87.83%

Table 11
Robustness analysis for different parameter combinations for an initial budget of $20 million available over two planning horizons of length $T = 10$ years and $T = 20$ years. Negative values are enclosed in parentheses.

Planning horizon, T	Percentage energy saving in cooling degree- hours by GRs, α	Percentage energy saving in heating degree- hours by GRs, β	Percentage efficiency increase in PV panel output, θ	Z^* (USD)	$\tilde{Z}$ (USD)	$\tilde{O}$ (USD)
10	10%	-10%	2.5%	(642,680,064)	(642,306,584)	373,480
			7.5%	(642,680,064)	(642,306,584)	373,480
		10%	2.5%	(644,895,574)	(642,680,064)	2,215,510
			7.5%	(644,895,574)	(642,680,064)	2,215,510
	20%	-10%	2.5%	(642,680,064)	(642,405,147)	274,917
			7.5%	(642,680,064)	(642,405,147)	274,917
		10%	2.5%	(645,583,951)	(642,680,064)	2,903,887
			7.5%	(645,583,951)	(642,680,064)	2,903,887
20	10%	-10%	2.5%	(2,441,792,744)	(2,437,914,658)	3,878,086
			7.5%	(2,442,331,322)	(2,438,457,551)	3,873,771
		10%	2.5%	(2,446,274,934)	(2,441,402,503)	4,872,431
			7.5%	(2,446,791,546)	(2,441,792,744)	4,998,802
	20%	-10%	2.5%	(2,441,792,744)	(2,439,849,247)	1,943,497
			7.5%	(2,442,412,330)	(2,440,445,560)	1,966,770
		10%	2.5%	(2,453,838,358)	(2,441,483,511)	12,354,847
			7.5%	(2,454,220,178)	(2,441,792,744)	12,427,434

Table 12
Total amount of requisite fossil fuels to produce the electricity saved and/or generated under the optimal solution in Cases 1–3 for two planning horizons of length $T = 10$ years and $T = 20$ years.

	$T = 10$			$T = 20$		
	Coal (kg)	Natural gas (m^3)	Oil (m^3)	Coal (kg)	Natural gas (m^3)	Oil (m^3)
Case 1	101,275	44,104	61	1,747,690	761,092	1044
Case 2	101,275	44,104	61	176,663,933	76,934,444	105,564
Case 3	101,275	44,104	61	179,670,700	78,243,845	107,361

tion. In this section, we conduct robustness analysis to investigate the impact of parameter misspecification on the solution. Specifically, we evaluate the robustness of the model with respect to parameters α, β, and θ, for $T = 10$ and $T = 20$ years, and provide the expected loss of profit due to parameter misspecification.

Let Z^* denote the total profit generated in USD given the true parameter settings. Let $\hat{Z}$ denote the total profit generated in USD from executing the model under extreme parameter misspecifications. Recall that Table 2 provides the estimated parameter ranges and levels used in the study. Hence, $\hat{Z}$ gives the total profit generated when a subset of parameters have been misspecified in the extreme, i.e., the parameters of interest assume their maximum (minimum) values as reported in Table 2, while the true parameter values are at their minimum (maximum). We let $\hat{x_i^k}$, $\hat{y_i^k}$, and $\hat{k_i^k}$ denote the corresponding solution. Now let $\tilde{Z}$ denote the total profit in USD when the solution $\hat{x_i^k}$, $\hat{y_i^k}$, and $\hat{k_i^k}$ is evaluated under the true parameter values. Lastly, let $\tilde{O}$ denote the cost of misspecifying the parameters, i.e., $\tilde{O} = Z^* - \tilde{Z}$.

Table 11 presents the robustness analysis results on the three parameters of percentage energy saving in cooling degree-hours due to GR installation, α, percentage energy saving in heating degree-hours due to GR installation, β, and percentage efficiency increase in the output of PV panels due to integration with GRs, θ, for an initial budget of $20 million available over two planning horizons of length $T = 10$ years and $T = 20$ years. The parameters α, β, and θ are particularly chosen as they are generally difficult to estimate and are functions of many other factors themselves, such as the type of GR vegetation, the GR isolation layer, and the climate. As seen in Table 11, the lost opportunity, $\tilde{O}$, ranges between $275 thousand and $12.4 million. Note that for $T = 10$, the values of $\tilde{O}$ are not impacted by the change in the value of θ as no PV panel is installed in these cases. Overall, despite the significant difference among the values of $\tilde{O}$ in the table, this difference is somewhat small with respect to θ, when all other parameters are held constant. The values of $\tilde{O}$ are in general most sensitive with respect to the parameters α, and especially β, and hence, care needs to be taken when calibrating these parameters for an investment in a particular climatic region.

4.5. Environmental insights

Recall that the goal of the model is to maximize the overall *profit* from energy generated and/or saved across a set of regions by investing in PV systems and/or GRs. In this section, we discuss the environmental implications of such an investment and provide insights on the benefits achievable by the implementation of the proposed model.

Table 12 presents the positive impact of implementing the optimal solutions provided for the three cases introduced in Table 5, for $T = 10$ years and $T = 20$ years, from an environmental perspective. Specifically, Table 12 presents the amount of fossil fuels needed [39] to produce the amount of electricity that is generated and/or saved through the implementation of the solutions provided in Table 6, after accounting for the required energy for manufacturing, distribution, and end-of-life processing of installed PV panels [3,9,44,55]. Note that the corresponding required energy for GRs are negligible [15]. (Please see Appendix D for more detail.)

For instance, consider Case 3 in Table 6. When $T = 20$ years, it is optimal to install 4735m^2 stand-alone GRs and 93,930 m^2 GR integrated PV panels. As shown in Table 12, implementing this solution in the City of Knoxville achieves approximately 179.7 million kg reduction in coal usage, or equivalently, 78.2 million m^3 or 107.4 thousand m^3 reduction in natural gas or oil usage, respectively. According to [40], these values translate into approximately

372 million kg, 152 million kg, and 309 million kg decrease in CO_2 emissions, respectively.

5. Conclusion and remarks

In this study, we evaluate the overall profit from energy generated and saved through installation of PV panels and GRs, while incorporating future climate uncertainties and the interaction between the practices. We study the model over two different planning horizon lengths, $T = 10$ and $T = 20$ years. The results suggest that a 10-year planning horizon is generally too short to allow for a profitable investment. However, a 20-year planning horizon, which is also more consistent with the lifespans of PV panels and GRs, is a better time frame for evaluating the outcomes of an investment on these green technologies. The results also show the importance of incorporating the PV-GR integration efficiency increase as it can significantly change the optimal solutions. The sensitivity analysis demonstrates that different cost and output of PV panels can significantly change the optimal solution. The sensitivity and robustness analyses show that the model is sensitive with respect to GR-related parameters, suggesting the need for careful calibration of these parameters before large scale implementation in any climate region. Lastly, the results indicate that considering the long-term changes in the rate of energy consumption affects the distribution of budget/rooftop areas between PV panels and GRs.

In this study, we only focus on the energy savings provided by GRs. Future studies may also incorporate other beneficial aspects of utilizing GRs in an urban area (such as run-off reduction, scaling down CO_2 emissions, and heat island mitigation) to more accurately evaluate the overall benefits of installing GRs and their significant role in increasing the urban resiliency. In addition, although the developed model is capable of considering multiple regions, due to limited data availability, especially with regard to future climate projections, in this study we only focus on one region, i.e., Knoxville, Tennessee. Future studies may include using this model to evaluate investment options across multiple regions with different climates.

Acknowledgments

The authors thank Jon M. Hathaway and Thom Epps for assisting with data collection and extraction, and providing insights. We also thank the editor and reviewers for their constructive and helpful comments. This work was supported in part by the National Science Foundation Grant CMMI-1634975.

Supplementary material

Supplementary material associated with this article can be found, in the online version, at 10.1016/j.omega.2018.10.016

References

[1] Abdelaziz FB, Aouni B, El Fayedh R. Multi-objective stochastic programming for portfolio selection. Eur J Oper Res 2007;177(3):1811–23.
[2] Albareda-Sambola M, Fernández E, Saldanha-da Gama F. The facility location problem with bernoulli demands. Omega (Westport) 2011;39(3):335–45.
[3] Alsema EA, Nieuwlaar E. Energy viability of photovoltaic systems. Energy Policy 2000;28(14):999–1010.
[4] Amato AD, Ruth M, Kirshen P, Horwitz J. Regional energy demand responses to climate change: methodology and application to the commonwealth of massachusetts. Clim Change 2005;71(1–2):175–201.
[5] Ampim PA, Sloan JJ, Cabrera RI, Harp DA, Jaber FH. Green roof growing substrates: types, ingredients, composition and properties. J Environ Hortic 2010;28(4):244–52.
[6] Arnette AN. Integrating rooftop solar into a multi-source energy planning optimization model. Appl Energy 2013;111:456–67.
[7] Ascione F, Bianco N, de'Rossi F, Turni G, Vanoli GP. Green roofs in european climates. are effective solutions for the energy savings in air-conditioning? Appl Energy 2013;104:845–59.
[8] Aurora Energy a. Peak Sun Hours; 2018. http://www.aurorasolarenergy.com/average-daily-sun-hours/
[9] Bankier C, Gale S. Energy Payback of Roof Mounted Photovoltaic Cells; 2006.
[10] Banos R, Manzano-Agugliaro F, Montoya F, Gil C, Alcayde A, Gómez J. Optimization methods applied to renewable and sustainable energy: a review. Renew Sustain Energy Rev 2011;15(4):1753–66.
[11] Barbarosogu G, Arda Y. A two-stage stochastic programming framework for transportation planning in disaster response. JOperResSoc 2004;55(1):43–53.
[12] BCC. Beijing Climate Center, China Meteorological Administration; 2017. http://forecast.bcccsm.ncc-cma.net/web/channel-1.htm
[13] Belzer DB. Energy Efficiency Potential in Existing Commercial Buildings: Review of Selected Recent Studies. Tech. Rep.. Pacific Northwest National Lab. (PNNL), Richland, WA (United States); 2009.
[14] Berndtsson JC. Green roof performance towards management of runoff water quantity and quality: a review. Ecol Eng 2010;36(4):351–60.
[15] Bianchini F, Hewage K. How "green" are the green roofs? lifecycle analysis of green roof materials. Build Environ 2012;48:57–65.
[16] Birge JR, Louveaux F. Introduction to stochastic programming. Springer Science & Business Media; 2011.
[17] Bose BK. Global warming: energy, environmental pollution, and the impact of power electronics. Ind Electron Mag, IEEE 2010;4(1):6–17.
[18] Boston Solar b. Solar panels - lifetime productivity and maintenance costs; 2018. http://www.bostonsolar.us/solar-blog-resource-center/blog/solar-panels-lifetime-productivity-and-maintenance-costs/
[19] Burroughs H, Hansen SJ. Managing indoor air quality fifth edition, 1. CRC Press; 2013.
[20] CCSI. Oak Ridge National Laboratory's Climate Change Science Institute; 2017. https://ccsi.ornl.gov
[21] Census Bureau US. Median and average square feet of floor area in new single-family houses completed by location; 2018. https://www.census.gov/const/C25Ann/sftotalmedavgsqft.pdf
[22] Census Bureau US. Number of Stories in New Single-Family Houses Completed; 2018. https://www.census.gov/construction/chars/pdf/stories.pdf
[23] Chang N-B, Rivera BJ, Wanielista M. Cost benefit optimization of cistern volume and green roof area in the Florida Showcase Green Envirohome (FSGE). In: Sustainable Systems and Technology (ISSST), 2010 IEEE International Symposium on. IEEE; 2010. p. 1–6.
[24] Chemisana D, Lamnatou C. Photovoltaic-green roofs: an experimental evaluation of system performance. Appl Energy 2014;119:246–56.
[25] Chen S-G. Bayesian approach for optimal PV system sizing under climate change. Omega (Westport) 2013;41(2):176–85.
[26] Chow TT. A review on photovoltaic/thermal hybrid solar technology. Appl Energy 2010;87(2):365–79.
[27] Chung D, Davidson C, Fu R, Ardani K, Margolis R. US photovoltaic prices and cost breakdowns: Q1 2015 benchmarks for residential, commercial, and utility-scale systems. Tech. Rep.. NREL Technical Report, In Preparation; 2015.
[28] CMCC. Euro-Mediterranean Center on Climate C hange; 2017. http://www.cmcc.it/models/cmcc-cm
[29] Coma J, Pérez G, Solé C, Castell A, Cabeza LF. Thermal assessment of extensive green roofs as passive tool for energy savings in buildings. Renew Energy 2016;85:1106–15.
[30] Cook-Patton SC, Bauerle TL. Potential benefits of plant diversity on vegetated roofs: a literature review. J Environ Manage 2012;106:85–92.
[31] Correia I, Nickel S, Saldanha-da Gama F. A stochastic multi-period capacitated multiple allocation hub location problem: formulation and inequalities. Omega (Westport) 2018;74:122–34.
[32] CRONOS. Mc Ghee Tyson Airport (KTYS); 2017. http://climate.ncsu.edu/cronos/?station=KTYS
[33] CSIRO. ACCESS Climate Model; 2017. http://www.csiro.au/en/Research/OandA/Areas/Assessing-our-climate/CAWCR/ACCESS/
[34] Current Results Weather, Science Facts. Average annual sunshine by state; 2017. https://www.currentresults.com/Weather/US/average-annual-state-sunshine.php
[35] Degree Days Weather Data. Custom degree day data; 2017. http://www.degreedays.net
[36] Dunec JL. Banking on green: a look at how green infrastructure can save municipalities money and provide economic benefits community-wide; 2012.
[37] EarthClim. Multi-institutional, coordinated climate research in Norway; 2017. http://folk.uib.no/ngfhd/EarthClim/
[38] EIA. Average price of electricity to ultimate customers by end-use sector; 2017. https://www.eia.gov/electricity/monthly/epm_table_grapher.cfm?t=epmt_5_6_a
[39] EIA. Average quality of fossil fuel receipts for the electric power industry; 2017. https://www.eia.gov/electricity/annual/html/epa_07_03.html
[40] EIA. Carbon dioxide uncontrolled emission factors; 2017. https://www.eia.gov/electricity/annual/html/epa_a_03.html
[41] EIA. Residential Energy Consumption Survey (RECS); 2017. https://www.eia.gov/consumption/residential/
[42] EIA. Heating and cooling no longer majority of U.S. home energy use; 2018. https://www.eia.gov/todayinenergy/detail.php?id=10271&src=%E2%80%B9%20Consumption%20%20%20%20%20%20Residential%20Energy%20Consumption%20Survey%20(RECS)-f4
[43] EIA. Today in energy; 2018. https://www.eia.gov/todayinenergy/detail.php?id=14771
[44] EIA E. U.S. imports of solar photovoltaic modules mainly come from Asia; 2018. https://www.eia.gov/todayinenergy/detail.php?id=34952

[45] EIA EIA. Annual energy outlook 2015 with projections to 2040. Department of Energy; 2015.
[46] Energy Informative. The real lifespan of solar panels; 2017. http://energyinformative.org/lifespan-solar-panels/
[47] Energy Informative E. What's the difference between net metering and feed-in tariffs?; 2014. http://energyinformative.org/net-metering-feed-in-tariffs-difference
[48] Energy Saving Trust E. Solar Energy Calculator Sizing Guide; 2015. http://www.pvfitcalculator.energysavingtrust.org.uk/Documents/150224_SolarEnergy_Calculator_Sizing_Guide_v1.pdf
[49] EPA E. Incorporating Low Impact Development into Municipal Stormwater Programs; 2009. https://www3.epa.gov/region1/npdes/stormwater/assets/pdfs/IncorporatingLID.pdf
[50] EPA E. Wind energy development in region 8; 2017. https://www.epa.gov/sites/production/files/documents/WindEnergyDevelopmentInReg8Draft19Dec07.pdf
[51] Feed-in Tariffs f. What is the export tariff?; 2018. http://www.fitariffs.co.uk/fits/principles/export/
[52] Feldman D, Barbose G, Margolis R, James T, Weaver S, Darghouth N, et al. Photovoltaic system pricing trends: historical, recent, and near-term projections. 2014 edition. Presentation by SunShot, US Department of Energy, NREL/PR-6A20-62558; 2014.
[53] Feng H, Hewage K. Energy saving performance of green vegetation on LEED certified buildings. Energy Build 2014;75:281–9.
[54] Florida Solar Energy Center F. Cell, modules, and arrays; 2018. http://www.fsec.ucf.edu/en/consumer/solar_electricity/basics/cells_modules_arrays.htm
[55] Frischknecht R, Itten R, Sinha P, de Wild-Scholten M, Zhang J, Fthenakis V, et al. Life cycle inventories and life cycle assessment of photovoltaic systems. Int. Energy Agency (IEA) PVPS Task 2015;12(9).
[56] Gagnon P, Margolis R, Melius J, Phillips C, Elmore R. Rooftop solar photovoltaic technical potential in the united states: a detailed assessment. Rep No NREL/TP-6A20-65298) Retrieved March 2016;30:2016.
[57] Gargari C, Bibbiani C, Fantozzi F, Campiotti CA. Simulation of the thermal behaviour of a building retrofitted with a green roof: optimization of energy efficiency with reference to italian climatic zones. Agric Agric Sci Procedia 2016;8:628–36.
[58] Gou B. Generalized integer linear programming formulation for optimal pmu placement. IEEE Trans Power Syst 2008;23(3):1099–104.
[59] Green HM, Kozek AS. Modelling weather data by approximate regression quantiles.. ANZIAM Journal 2003;44:229–48.
[60] Green Infrastructure Foundation g. Making informed decisions: a green roof cost and benefit study for Denver; 2017. https://static1.squarespace.com/static/588221e420099e47b8fe06d8/t/59e0e8d0017db2106c37d7b5/1507911889792/Denver_Cost_Benefit_Report_Final.pdf
[61] Green Roof Technology g. Solar garden roof – first, fully integrated solar and extensive green roof; 2018. http://www.greenrooftechnology.com/Solar_PV_Greenroofs
[62] Griva I, Nash SG, Sofer A. Linear and nonlinear programming. Society for Industrial and Applied Mathematics, Philadelphia; 2009.
[63] GSA U.. The benefits and challenges of green roofs on public and commercial buildings. A Report of the United States General Service Administration2011.
[64] GSA U.G.S.A.. The benefits and challenges of green roofs on public and commercial buildings. 2011.
[65] Gurobi O. Inc.,"gurobi optimizer reference manual," 2015. Google Scholar; 2014.
[66] Hand MM. Renewable electricity futures study. National Renewable Energy Laboratory; 2012.
[67] Hoffert MI, Caldeira K, Jain AK, Haites EF, Harvey LD, Potter SD, et al. Energy implications of future stabilization of atmospheric CO2 content. Nature 1998;395(6705):881–4.
[68] Hong T, Koo C, Park J, Park HS. A gis (geographic information system)-based optimization model for estimating the electricity generation of the rooftop pv (photovoltaic) system. Energy 2014;65:190–9.
[69] Hostick DJ, Belzer DB, Hadley SW, Markel T, Marnay C, Kintner-Meyer MC. Projecting Electricity Demand in 2050. Tech. Rep.. Pacific Northwest National Laboratory (PNNL), Richland, WA (United States); 2014.
[70] Huang Y.. The impact of climate change on the energy use of the US residential and commercial building sectors. Lawrence Berkeley National Laboratory, Tech. Rep.Report No. LBNL-60754 2006.
[71] Hui SC, Chan S. Integration of green roof and solar photovoltaic systems. In: Joint symposium; 2011. p. 1–12.
[72] IGRA. International Green Roof Association; 2017. http://www.igra-world.com/types_of_green_roofs/
[73] IPCC. Intergovermental Panel on Climate Change Data Distribution Centre; 2017. http://www.ipcc-data.org/guidelines/pages/gcm_guide.html
[74] IPSL. Institut Pierre Simon Laplace Climate Modeling Center; 2017. http://icmc.ipsl.fr/
[75] JMA. Japan Meteorological Agency; 2017. http://ds.data.jma.go.jp/tcc/tcc/products/gwp/gwp7/html_e/model.html
[76] Jun M, Knutti R, Nychka DW. Spatial analysis to quantify numerical model bias and dependence: how many climate models are there? J Am Stat Assoc 2008;103(483):934–47.
[77] Kasper M, Bortis D, Kolar JW. Classification and comparative evaluation of pv panel-integrated dc–dc converter concepts. IEEE Trans Power Electron 2014;29(5):2511–26.
[78] Kim J, Hong T, Koo C-W. Economic and environmental evaluation model for selecting the optimum design of green roof systems in elementary schools. Environ SciTechnol 2012;46(15):8475–83.
[79] Kodysh JB, Omitaomu OA, Bhaduri BL, Neish BS. Methodology for estimating solar potential on multiple building rooftops for photovoltaic systems. Sustainable Cities Soc 2013;8:31–41.
[80] Köhler M, Wiartalla W, Feige R. Interaction between PV-systems and extensive green roofs. In: Proceedings of the fifth annual greening rooftops for sustainable communities conference, awards and trade show; 2007.
[81] Koo C, Hong T, Lee M, Kim J. An integrated multi-objective optimization model for determining the optimal solution in implementing the rooftop photovoltaic system. Renewable Sustainable Energy Rev 2016;57:822–37.
[82] Kornelakis A. Multiobjective particle swarm optimization for the optimal design of photovoltaic grid-connected systems. Sol Energy 2010;84(12):2022–33.
[83] LASG. Institute of Atmospheric Physics, State Key Laboratory of Numerical Modeling for Atmospheric Sciences and Geophysical Fluid Dynamics; 2017. http://www.lasg.ac.cn/
[84] Levinson R, Akbari H, Pomerantz M, Gupta S. Solar access of residential rooftops in four california cities. Sol Energy 2009;83(12):2120–35.
[85] Li Y, Babcock RW. Green roof hydrologic performance and modeling: a review. Water Sci Technol 2014;69(4):727–38.
[86] Liu G, Rasul M, Amanullah M, Khan MMK. Techno-economic simulation and optimization of residential grid-connected PV system for the queensland climate. Renew Energy 2012;45:146–55.
[87] Loveland J, Brown G. Impacts of climate change on the energy performance of buildings in the united states; 1996.
[88] Mansur E, Mendelsohn R, Morrison W. A Discrete-continuous Choice Model of Climate Change Impacts on Energy; 2005.
[89] Maqsood I, Huang GH. A two-stage interval-stochastic programming model for waste management under uncertainty. J Air Waste Manage Assoc 2003;53(5):540–52.
[90] Marmidis G, Lazarou S, Pyrgioti E. Optimal placement of wind turbines in a wind park using monte carlo simulation. Renew Energy 2008;33(7):1455–60.
[91] Minnesota Stormwater Manual m. Cost-benefit considerations for green roofs; 2018. https://stormwater.pca.state.mn.us/index.php?title=Cost-benefit_considerations_for_green_roofs
[92] MPI. New earth system model of max planck institute for meteorology; 2017. http://www.mpimet.mpg.de/en/science/models/mpi-esm.html
[93] NCAR. CESM models; 2017. http://www.cesm.ucar.edu/models/ccsm4.0//
[94] Niachou A, Papakonstantinou K, Santamouris M, Tsangrassoulis A, Mihalakakou G. Analysis of the green roof thermal properties and investigation of its energy performance. Energy Build 2001;33(7):719–29.
[95] Noyan N. Risk-averse two-stage stochastic programming with an application to disaster management. Comput Oper Res 2012;39(3):541–59.
[96] Ordóñez J, Jadraque E, Alegre J, Martínez G. Analysis of the photovoltaic solar energy capacity of residential rooftops in andalusia (spain). Renewable Sustainable Energy Rev 2010;14(7):2122–30.
[97] Parisio A, Jones CN. A two-stage stochastic programming approach to employee scheduling in retail outlets with uncertain demand. Omega (Westport) 2015;53:97–103.
[98] Park HS, Jeong K, Hong T, Ban C, Koo C, Kim J. The optimal photovoltaic system implementation strategy to achieve the national carbon emissions reduction target in 2030: focused on educational facilities. Energy Build 2016;119:101–10.
[99] Porsche U., Köhler M.. Life cycle costs of green roofs. World Climate & Energy Event2013;.
[100] Princeton University. Geophysical Fluid Dynamics Laboratory; 2017. https://www.gfdl.noaa.gov/earth-system-model/
[101] Raji B, Tenpierik MJ, van den Dobbelsteen A. The impact of greening systems on building energy performance: a literature review. Renewable Sustainable Energy Rev 2015;45:610–23.
[102] Refahi AH, Talkhabi H. Investigating the effective factors on the reduction of energy consumption in residential buildings with green roofs. Renew Energy 2015;80:595–603.
[103] Rehman S, Bader MA, Al-Moallem SA. Cost of solar energy generated using PV panels. Renewable Sustainable Energy Rev 2007;11(8):1843–57.
[104] Rosenthal DH, Gruenspecht HK, Moran EA. Effects of global warming on energy use for space heating and cooling in the united states. Energy J 1995:77–96.
[105] Ruth M, Lin A-C. Regional energy demand and adaptations to climate change: methodology and application to the state of maryland, USA. Energy Policy 2006;34(17):2820–33.
[106] Sailor DJ. Relating residential and commercial sector electricity loads to climate–evaluating state level sensitivities and vulnerabilities. Energy 2001;26(7):645–57.
[107] Sailor DJ, Pavlova A. Air conditioning market saturation and long-term response of residential cooling energy demand to climate change. Energy 2003;28(9):941–51.
[108] Santamouris M. Cooling the cities–a review of reflective and green roof mitigation technologies to fight heat island and improve comfort in urban environments. Sol Energy 2014;103:682–703.
[109] Scherba A, Sailor DJ, Rosenstiel TN, Wamser CC. Modeling impacts of roof reflectivity, integrated photovoltaic panels and green roof systems on sensible heat flux into the urban environment. Build Environ 2011;46(12):2542–51.

Please cite this article as: M. Ramshani, A. Khojandi and X. Li et al., Optimal planning of the joint placement of Photovoltaic panels and green roofs under climate change uncertainty, Omega, https://doi.org/10.1016/j.omega.2018.10.016

[110] Schneising O, Reuter M, Buchwitz M, Heymann J, Bovensmann H, Burrows J. Terrestrial carbon sink observed from space: variation of growth rates and seasonal cycle amplitudes in response to interannual surface temperature variability. Atmos Chem Phys 2014;14(1):133–41.
[111] Scott MJ, Dirks JA, Cort KA. The Adaptive Value of Energy Efficiency Programs in a Warmer World. Tech. Rep.. Pacific Northwest National Lab.(PNNL), Richland, WA (United States); 2005.
[112] SEIA SEIA. Net Metering; 2018. https://www.seia.org/initiatives/net-metering
[113] Snodgrass EC, Snodgrass LL. Green roof plants: a resource and planting guide 04; SB419. 5, S5. Timber Press Portland; 2006.
[114] Solar Direct. Solar electric system sizing; 2017. http://www.solardirect.com/pv/systems/gts/gts-sizing-sun-hours.html
[115] Solar Power Authority s. How to calculate your peak sun-hours; 2018. https://www.solarpowerauthority.com/how-to-calculate-your-peak-sun-hours/
[116] Solar Quotes. Inverters; 2017. https://www.solarquotes.com.au/inverters/
[117] Sonne J. Evaluating green roof energy performance. Ashrae J 2006;48(2):59.
[118] Spala A, Bagiorgas H, Assimakopoulos M, Kalavrouziotis J, Matthopoulos D, Mihalakakou G. On the green roof system. selection, state of the art and energy potential investigation of a system installed in an office building in athens, greece. Renew Energy 2008;33(1):173–7.
[119] SVS. Renewable solutions; 2017. http://www.svsolar.com/projects/harned.htm
[120] The City of Knoxville C. 2017–2018 Budget; 2018. http://www.knoxvilletn.gov/government/city_departments_offices/Finance/budget/budget_archive/2017-2018_budget/
[121] Tyagi V, Rahim NA, Rahim N, Jeyraj A, Selvaraj L. Progress in solar pv technology: research and achievement. Renewable Sustainable Energy Rev 2013;20:443–61.
[122] UDI. Oak Ridge National Laboratory's Urban Dynamics Institute; 2017. https://udi.ornl.gov
[123] Van Hoesen J, Letendre S. Evaluating potential renewable energy resources in poultney, vermont: a gis-based approach to supporting rural community energy planning. Renew Energy 2010;35(9):2114–22.
[124] Van Slyke RM, Wets R. L-shaped linear programs with applications to optimal control and stochastic programming. SIAM J Appl Math 1969;17(4):638–63.
[125] Wang C, Nehrir MH. Analytical approaches for optimal placement of distributed generation sources in power systems. IEEE Trans Power Syst 2004;19(4):2068–76.
[126] Whaley C. Best practices in photovoltaic system operations and maintenance. Tech. Rep.. National Renewable Energy Lab.(NREL), Golden, CO (United States); 2016.
[127] Wholesale Solar W. Power inverters; 2018. https://www.wholesalesolar.com/power-inverters
[128] Wiese S, Libby L, Energy A, Long E, Ryan B. A solar rooftop assessment for Austin. SOLAR 2010 conference proceedings. Phoenix AZ; 2010.
[129] Witmer L. Quantification of the passive cooling of photovoltaics using. The Pennsylvania State University; 2010. Ph.D. thesis.
[130] Witmer L, Brownson J. An energy balance model of green roof integrated photovoltaics: a detailed energy balance including microclimatic effects. In: ASES; 2011. p. 17–21.
[131] Wong E., Akbari H., Bell R., Cole D.. Reducing urban heat islands: compendium of strategies. Environmental Protection Agency, retrieved May 2011; 12:2011.
[132] Yang C-J. Reconsidering solar grid parity. Energy Policy 2010;38(7):3270–3.
[133] Yang J, Yu Q, Gong P. Quantifying air pollution removal by green roofs in chicago. Atmos Environ 2008;42(31):7266–73.
[134] Yongqiang Y, Xuehong Z, Yufu G. Global coupled ocean-atmosphere general circulation models in LASG/IAP. Adv Atmos Sci 2004;21(3):444–55.
[135] Zhao M, Srebric J. Assessment of green roof performance for sustainable buildings under winter weather conditions. J Central South Univ 2012;19(3):639–44.
[136] Zhou Z, Zhang J, Liu P, Li Z, Georgiadis MC, Pistikopoulos EN. A two-stage stochastic programming model for the optimal design of distributed energy systems. Appl Energy 2013;103:135–44.

Please cite this article as: M. Ramshani, A. Khojandi and X. Li et al., Optimal planning of the joint placement of Photovoltaic panels and green roofs under climate change uncertainty, Omega, https://doi.org/10.1016/j.omega.2018.10.016